Review of aeronautical fatigue and structural integrity investigations in the UK during the period April 2015 - April 2017

Reed, S. C. and Hallam, D.

DSTL/TR102138 Ver 2
27 April 2017

Dstl
Platform Systems Division
Porton Down
Salisbury
Wilts
SP4 0JQ

Release Conditions

This document has been compiled by Dstl but contains information released by each author's organisation for presentation to the International Committee on Aeronautical Fatigue and Structural Integrity (ICAF), 2017.

Executive summary

This review is a summary of the aeronautical fatigue and structural integrity investigations carried out in the United Kingdom during the period April 2015 to April 2017. The review has been compiled for presentation at the 35th Conference of the International Committee on Aeronautical Fatigue and Structural Integrity (ICAF), to be held in Nagoya, Japan in June 2017.

The contributions generously provided by colleagues from within the aerospace industry and universities are gratefully acknowledged. The names of contributors and their affiliation are shown below the title of each item.

Table of contents

1 Introduction

This review is a summary of the aeronautical fatigue and structural integrity investigations carried out in the United Kingdom during the period April 2015 to April 2017. The review has been compiled for presentation at the 35th Conference of the International Committee on Aeronautical Fatigue and Structural Integrity (ICAF), to be held in Nagoya, Japan in June 2017.

The contributions generously provided by colleagues from within the aerospace industry and universities are gratefully acknowledged. The names of contributors and their affiliation are shown below the title of each item.

The format of the paper is similar to that of recent UK ICAF reviews; the topics covered include:

- Full scale fatigue testing
- Enhancing fatigue performance
- Fatigue performance of novel manufacturing methods
- Development in fatigue design and structural lifing tools
- Non-destructive evaluation
- Corrosion protection and prevention
- Structural integrity assurance
- Developments in fatigue, usage and structural health monitoring

References are annotated at the end of each contribution and are self-contained within the contribution. Figure and table numbers are also self-contained within the contribution.

Intentionally Blank

2 Full scale fatigue testing

2.1 Use of full scale fatigue test results to produce accurate fatigue life predictions: lessons learned

K. Shehzad-Saleem[1], M. Alessandro[1], D. Dort[2], [1]Airbus Operations Limited, United Kingdom, [2]Airbus Operations GmbH, Germany

This entry is an abstract. The full paper can be found in the ICAF2017 proceedings.

For the determination of maintenance requirements of primary structural elements, aircraft Type Certification relies on a number of conservative assumptions and coupon-based test data.

The objective of a full scale fatigue test (FSFT) is to verify how the aircraft structure responds to stress over a long period of time and during different stages of its operations. To recreate these conditions, a combination of loads is placed on the airframe and activated by computer-operated hydraulic jacks. This paper deals with the analysis and the interpretation of the test data and comparison with the analytical assessments.

A stress factor known as 'TRF' – Test to Result Factor is generated as the first step of the analysis. The TRF represents the calibration between the test and the analytical approach such as FE (Finite Element) linear simulations. The TRF is utilized in two stages: a TRFF for assessment of fatigue life and TRFCP for crack propagation. This paper takes into the account different geometrical factors (e.g. fastener hole diameter and stack thickness) of the structure and their relative influence on the TRF. By clustering the test findings an equivalent fatigue life of the local structural features can be calculated; each cluster comprises of the whole range of early and late initiations, adjusted with appropriate factors.

As a part of the statistical analysis NIL findings are also included in the statistical population, resulting in a correlated fatigue life of the local feature, from which a TRFF may be calculated. TRFCP uses a variety of test crack propagation data (striations counting of artificial cracks and natural damage growth etc.) and adjusts the geometrical Stress Intensity Factor (SIF).

This paper shows how the factors TRFF and TRFCP can be determined through the assessment of FSFT results, and how these results can be used to refine the maintenance inspection requirements for a wide-body aircraft.

3 Enhancing fatigue performance

3.1 Laser peening of aerospace aluminium alloys

M. E. Fitzpatrick, M. Pavan, S. Zabeen, N. Smyth, Coventry University

Laser shock peening (LSP) is a surface treatment that has been shown to increase the fatigue life of safety critical components and structures. This is achieved through introduction into the material of a compressive residual stress field that counteracts applied tensile stresses and thus reduces the applied stress intensity factor range. Research at Coventry University is currently being conducted to study the effect of LSP processing parameters such laser energy, spot size, spot overlapping distance etc. on the induced residual stress field. Work is also being done to understand the effect that LSP-induced residual stress has on the fatigue crack growth rate using both experimental and modelling approaches. This work is being done in partnership with Cranfield University, Universidad Politécnica de Madrid, US Air Force Research Laboratory, Alcoa Inc., Airbus GmbH, Metal Improvement Company, LSPT, University of Cincinnati, and University of the Witwatersrand.

Shown in Figure 1(A) is residual stress measured in the loading direction of a 2.5-mm-thick structural joint using angle dispersive XRD at the Advanced Photon Source in Chicago. LSP was applied to both faces of the sample in a patch across the first line of rivet holes, as illustrated in the figure, noting only the bottom half of the joint is shown for clarity. The residual stress field was measured between two of the rivet holes and was approximately 150 MPa in compression at the surfaces with the compressive field extending approximately 600 μm from the surface. However tensile balancing residual stress of magnitude averaging 100 MPa was measured in the centre of the sample. The effect of through-thickness variation of residual stress on fatigue crack growth and crack front shape evolution is currently an active area of research at Coventry University. In the case of the structural joint, LSP was found to increase the fatigue life compared with un-peened samples despite the balancing tensile residual stress field.

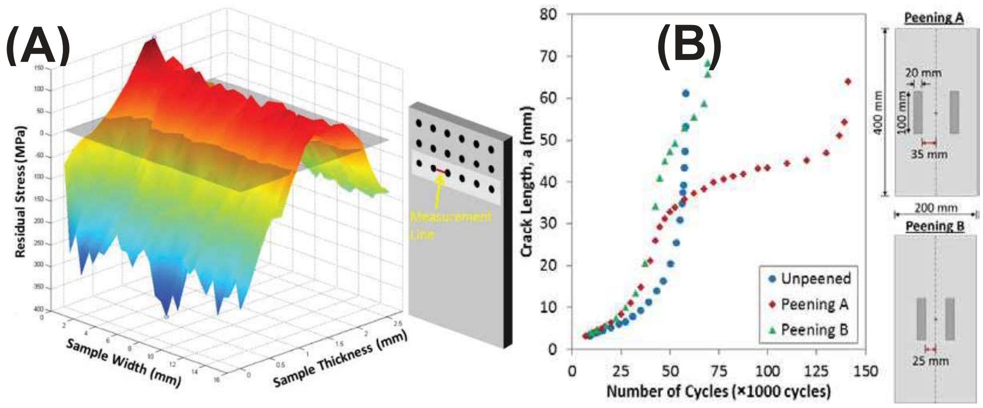

Figure 1: (A) Residual stress in the loading direction of a structural joint measured using angle dispersive XRD at the Advanced Photon Source, USA and (B) the effect on fatigue crack growth in an M(T) sample of the distance from the notch tip of a laser peened patch

Figure 1:(B) is the effect of LSP patch location on crack growth in an M(T) sample compared with baseline data

Peening A had the patch located 35 mm from the sample centreline and for peening B the patch was located 25 mm away, as illustrated in the figure. The LSP process parameters were consistent in each case and peening was applied to both faces of the samples. Both peening treatments resulted in an increased fatigue life compared with the baseline however for both cases the fatigue crack initially grew faster than the baseline crack. This was due to balancing tensile residual stress, measured using incremental hole drilling, outside the compressive peened patch. Once the crack reached the peened area, and hence the compressive residual stress field, the growth rate slowed. However for peening case A when the crack entered the peened region the stress intensity factor range was so great that the compressive residual stress had negligible effect on the fatigue life compared with peening case B. This work again highlights the importance of consideration of balancing tensile residual stress but also that optimal positioning of the peened patch is critical to optimise fatigue lie.

3.1.1 Conference Presentations

Pavan, M., Fitzpatrick, M.E., ‘Evaluation of Residual Stress in a 2050-T84 Aluminium plate after Laser Shock Peening’, presented at the 6th International Conference on Laser Peening and Related Phenomena, 6-11 November 2016, South Africa.

Smyth, N., Fitzpatrick, M.E., ‘A Parametric Study of the Effect of LSP Processing Parameters on the Induced Residual Stress Field in Aluminium 2624-T39’, presented at the 6th International Conference on Laser Peening and Related Phenomena, 6-11 November 2016, South Africa.

3.1.2 Publications

Pavan, M., Fitzpatrick, M.E. (2017) Evaluation of Residual Stress in a 2050-T84 Aluminium plate after Laser Shock Peening, International Journal of Structural Integrity. (submitted).

Toparli, M.B., Smyth, N., Fitzpatrick, M.E. (2017) Effect of treatment area on residual stress and fatigue in laser peened aluminum sheets. Metallurgical and Materials Transactions A: Physical Metallurgy and Materials Science. (article in press).

Toparli, M.B., Fitzpatrick, M.E. (2016). Development and application of the contour method to determine the residual stresses in thin laser-peened aluminium alloy plates. Experimental Mechanics, 56(2), 323-330.

3.2 Bonded crack retarders for aerospace aluminium alloys: effect of operation temperature

M.E. Fitzpatrick, A.K. Syed, Coventry University

This research has focused on improving the fail-safety of integral metallic structures by application of the bonded crack retarder (BCR) concept where a reinforcing material is adhesively bonded in critical locations to provide the local stiffening and crack bridging, thereby retarding the fatigue crack growth. Aluminium alloy 2624-T351 was used as the substrate and GLARE6/5 as the reinforcing strap (Fig. 2a). A high-temperature-cure adhesive, FM94, was used to bond the BCR. During this project, BCR performance when bonded on to small coupons, structural assemblies, and mock-up aircraft panels was investigated. The extensive experimental programme has shown that thermal residual stresses produced during the BCR bonding process are very low (~20 MPa) in all the coupon and structural assemblies. BCR has brought benefits to the fatigue crack growth rate (FCGR) and impact resistance properties [1]. A large part of the BCR programme was reported at the previous ICAF meetings [2] and publications [1, 3].

Since 2015, new analysis has been performed on the effect of temperature on the BCR performance [4]. During service, aircraft structures are exposed to a range of operating temperatures, from 70°C on the ground to −60°C at cruise altitudes. Continuous thermal cycling between these two extreme operating temperature values may influence the BCR performance. It is found that, for the high-damage-tolerant 2024 alloy: (1) although a single sided strap configuration can result in a 27% FCG life improvement at the room temperature (RT), little improvement in FCG rate is found when tested at 70°C and −60°C (Fig. 2b). For the 70°C test this is due to increased residual stress and secondary bending; both cause greater stress intensity factors. For the −60°C test, this is partly a consequence of the much reduced fatigue crack growth rate at −60°C (without straps), and much reduced residual stress and reversed secondary bending. (2) Thermal cycling prior to fatigue testing at room temperature does not impair the performance of the bonded crack retarders. There is no degradation in the properties of any of the components of the assembly resulting from exposure to the temperature extremes defined for the programme (Fig. 2c).

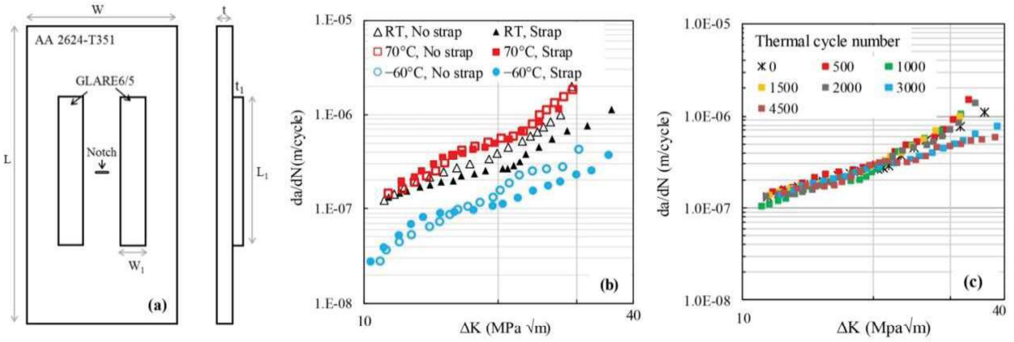

Fig 2. (a) M(T) specimen reinforced by GLARE straps, (b) fatigue crack growth rates tested at three temperatures, (c) effect of thermal cycling on crack growth rate tested at room temperature

[1] Syed AK , Fitzpatrick ME, Moffatt JE, Doucet J, Isidro Durazo-Cardenas, Effect of impact damage on the fatigue performance of structures reinforced with GLARE bonded crack retarders, Int J Fatigue 80 (2015): 231–237.

[2] UK National Reviews presented at ICAF2013.

[3] Syed AK, Fitzpatrick ME, Moffatt JE, Evolution of residual stress during fatigue crack growth in an aluminium specimen with a bonded crack retarder, Compos Struct 117 (2014): 12–16.

[4] Syed AK, Zhang X, Moffatt JE, Fitzpatrick ME. Effect of temperature and thermal cycling on fatigue crack growth in aluminium reinforced with GLARE bonded crack retarders. Int J Fatigue 98(2017): 53-61.

4 Fatigue performance of novel manufacturing methods

4.1 Additive manufactured Ti-6Al-4V titanium: fracture toughness, fatigue crack growth rate and model development

X. Zhang, A.K. Syed, Coventry University

In the Additive Manufacturing (AM, or 3D printing) research field, we have worked on titanium Ti-6Al-4V produced by the Wire + Arc Additive Manufacture (WAAM) process. The manufacture was conducted by Cranfield University's Welding Engineering and Laser Processing Centre led by Professor Stewart Williams. Following work has been performed:

Fracture toughness and effect of oxygen content and deposition orientation. Main conclusions are:

- Grade 23 Ti-6Al-4V (low oxygen content) has much greater fracture toughness (by 32%) than that of Grade 5 that is commonly used in the aerospace industry. However, grade 23 has much lower static strength.
- Both grades show higher toughness than that of a baseline wrought material.
- Fracture toughness is direction-dependent: it is slightly higher when a crack propagates across the additive layers compared to a crack aligned with the layers, meaning that there is more resistance to crack growth when it grows across the layer bands. For the grade 5 wire, the difference is within 3% (for the parallel deposition strategy) and 10% (for the oscillation deposition strategy). Explanation on the microstructure effect can be found in [1].

Fatigue crack growth rates in WAAM Ti-6Al-4V built by three different material deposition strategies (single path, parallel path and oscillation scanning) and two crack directions. Figure 3 shows crack growth rates in two material directions, i.e. crack across the additive layers, and crack along the layers. Key findings can be summarised as:

- Fatigue crack growth rate in WAAM Ti-6-4 is slower than that in baseline wrought plate, but faster than in the cast condition
- Crack growth rate is strongly direction-dependent when the crack growth driving force (the stress intensity factor range, SIF range) is less than 20 MPa√m. Crack growth rate is slower in the "across layers" case.
- Microstructure has played a significant role in this anisotropic behaviour. The alpha grain size varies within a layer band resulting in more resistance to crack growth when it is across the additive layer bands.
- Crack growth rate is fairly isotropic when the SIF range is greater than 20 MPa√m. Part of this work is published in [1]. Recent work on the effect of additive manufacture scanning strategies on crack growth life will be presented at the ICAF meeting [2].

Development of models for predicting fatigue crack growth life, incorporating characteristics of AM metals, e.g. anisotropic mechanical properties, residual stresses arising from repeated thermal cycles during the manufacture process, and defects in the forms of internal porosity and surface roughness. This analysis and characterisation work of mechanical performance, especially under fatigue loads, will contribute to product qualification and certification, and so promote the uptake of these technologies and new classes of materials.

In the models, the input residual stresses were measured by the contour method in a large as-build WAAM "wall". Further analysis was performed by FE modelling of residual stress release owing to cutting large WAAM panel into small lab specimens. Part of the modelling work was performed in collaboration with Dr Jikui Zhang of Beihang University (Beijing, China) via an academic exchange programme. Work is published in [3-4]. Figure 4 shows an example of an FE model of crack growth in an unsymmetrical residual stress field and along the interface of bi-material zones (to simulate additive material being deposited on to a wrought substrate in a practical design scenario, and cracking scenario from the interface).

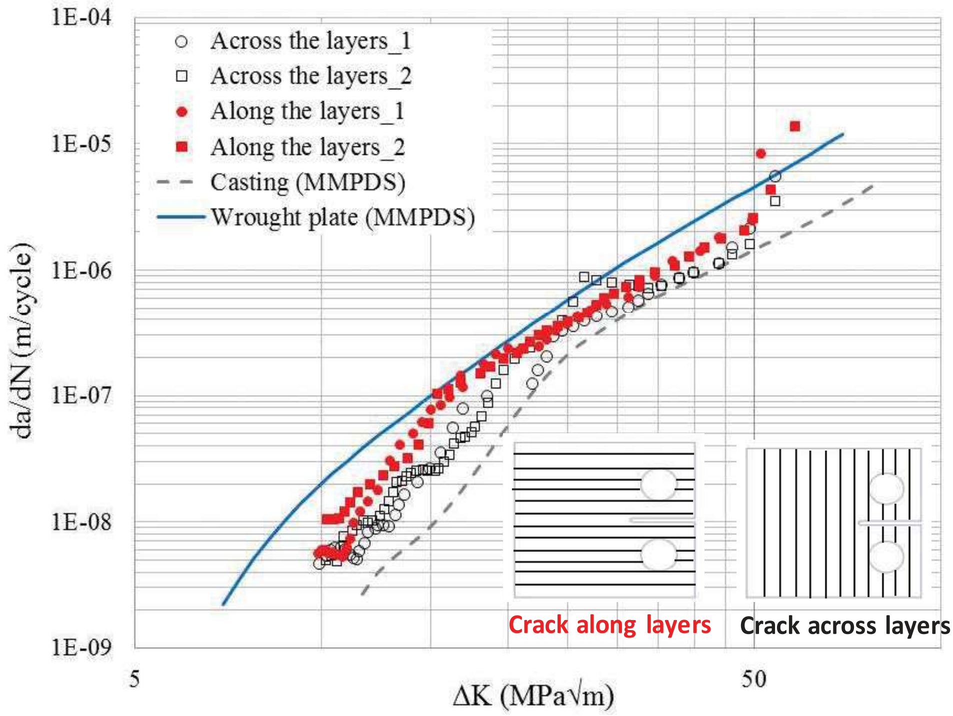

Figure 3: Fatigue crack growth rates in WAAM Ti-6Al-4V: influence of crack orientation (i.e. either across or along the additive deposited layers).

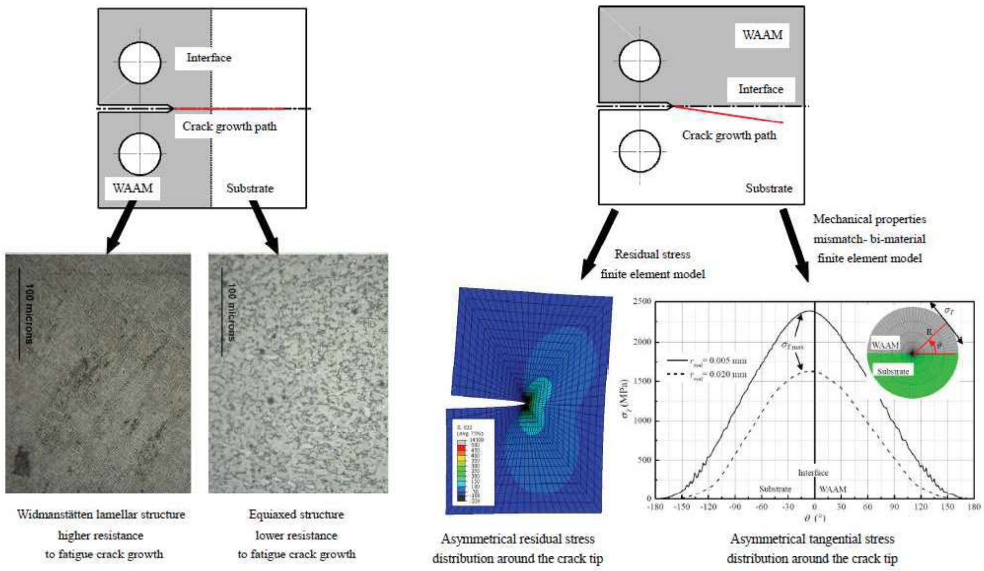

Figure 4: Fatigue crack growth behaviour at the interface between additive deposited and wrought metals: Left: crack propagating from AM to wrought alloy; microstructure dominates the crack growth rate; Right: crack started in parallel with the interface – it has the tendency to grow into the wrought alloy even it started inside the WAAM. This observation can be explained by FE modelling of unsymmetrical residual stress field, mismatch of the two yield strength, and crack growth rate of the two materials.

Publications [1-4] summarising the above described research. Work described in [2] will be presented at ICAF2017.

[1] Zhang X, Martina F, Ding J, Wang X, Williams SW. Fracture toughness and fatigue crack growth rate properties in wire + arc additive manufactured Ti-6Al-4V, Fatigue & Fract of Eng Mater & Struct. Nov 2016. Doi: 10.1111/ffe.12547.

[2] Zhang X, Syed, AK, Martina F, Ding J, Williams SW. Fatigue and Damage Tolerance Performance of Additive Manufactured Titanium: Control of residual stress and development of life evaluation method. Accept for presentation at ICAF2017, June 2017.

[3] Zhang J, Zhang X, Wang X, Ding J, Traoré Y, Paddea S, Williams SW, Crack path selection at the interface of wrought and wire + arc additive manufactured Ti-6Al-4V, Materials & Design, 104(2016) 365-375.

[4] Zhang J, Wang, X, Paddea, S, Zhang X. Fatigue crack propagation behaviour in wire+arc additive manufactured Ti-6Al-4V: effects of microstructure and residual stress, Materials & Design, 90(2016): 551-561.

4.2 Guidance on the qualification and certification of additive manufactured parts in military aviation

M. Lunt and R. Manghan, Defence Science and Technology Laboratory (Dstl)

The Military Aircraft Structural Airworthiness Advisory Group has initiated the development of guidance material for the qualification and certification of additive manufactured parts in military aviation. The aim is to focus on Grade A parts. A working group has been formed to contribute knowledge and to peer review the final document. The group contains representation from MBDA, BAE Systems, Airbus, Rolls-Royce, GKN, Leonardo Helicopters, Lockheed Martin, SAFRAN Landing Systems, SME AM Businesses, Civil Aviation Authority, National Physical Laboratory, Health and Safety Laboratory, AM Bureaux, Academia, MOD (MAA, 1710 Naval Air Squadron), Dstl, TWI, High Value Manufacturing Catapult and QinetiQ.

Much of the focus of the work is on understanding the sources of variation in performance of AM parts and their significance. When complete the document will be published on the UK Government Website, www.gov.uk, as MASAAG Paper 124.

5 Development in fatigue design and structural lifing tools

5.1 Aircraft Fatigue Analysis in the Digital Age

K. Graham, M. Artim and D. Daverschot, AIRBUS Structural Engineering

This entry is an abstract. The full paper can be found in the ICAF2017 proceedings.

Abstract: With the unending pursuit of efficiency by operators comes the requirement to continuously review the design and usage parameters of aircraft. Improved fatigue analysis offers a plethora of opportunities to provide not only benefits for design, but also tailored solutions on a case-by-case basis, including the optimisation of maintenance schedules without compromise to safety.

In order to unlock the full potential of a digital approach to fatigue, it is essential to take advantage of the huge volume of data now available, from meteorological conditions encountered to mission type flown. By applying a ‘big data’ mentality to more traditional analysis, limitless parameters will build a vast database of information to create the ‘Aircraft Fatigue Model’; operators will no longer be required to adhere to restrictions based on average fleet usage.

This paper discusses the strategy for moving aircraft fatigue analysis into the digital age, through the creation of the Aircraft Fatigue Model and digital twins, to the application of ‘big data’ analytics and the subsequent deliverables and benefits to operators unique to the digitalisation approach.

5.2 Developments in fatigue design tools – HBM Prenscia

A. Halfpenny and R. Plaskitt, HBM Prenscia

5.2.1 General Developments

HBM Prenscia [a] continues to develop their material fatigue testing capabilities and the fatigue damage models used in their nCode software products.

- The Advanced Materials Characterisation & Test laboratory (AMCT) has relocated from its historical location near Matlock, Derbyshire to a purpose built unit in the Advanced Manufacturing Park, Sheffield.
- AMCT laboratory performs tensile and fatigue tests of small coupon samples of metals, composites and polymers from -60 °C temperature to +1000 °C. Table 1 lists a sample of high strength and stainless steels, and aluminium, magnesium and titanium alloys that have been tested and characterised to strain-life mean curves, strain-life design curves (mean – 2 standard deviations) and stress-life curves.
- nCode DesignLife, for fatigue analysis from finite element analysis, has developed to support high performance computing clusters for large models, to include additional vibration fatigue environments, and to include static failure criteria and failure envelopes for composite materials (an extended abstract is included to describe this).
- nCode GlyphWorks, for fatigue analysis from measured strain (and general flight data processing), has developed to include structural dynamics (experimental modal analysis) and new data cleaning methods (Kalman filter, Wavelet denoising).
- New file format support includes common aerospace file formats: Curtiss-Wright PCAP (IENA), Dewesoft DXD, OROS OXF and Vector MDF

[a] HBM Prenscia is the new name for HBM-nCode, and includes the nCode software products for fatigue and durability analysis and the ReliaSoft software products for reliability engineering, life data analysis and FMEAs. For more details see: www.hbmprenscia.com

Steels	100Cr6	21CrMoV5-7	40CrNiMo
AISI 4140	AISI 4145H	AISI 4330V	ASTM B166 Inconel
BS Aerospace 5 S99	Ovako 225A	Ovako 277Q	Ovako 677
and many other mild and medium carbon steels			
Stainless Steel	13-8 PH Stainless	2205 Duplex	409 (L & T)
X2CrNiMo17-12-2	X5CrNi18-9	X6CrNiTi18-10	X8CrNiS18-9
Aluminium Alloys	1050-H14 (L & T)	2014-T651	2014A-T6511
2024	2024-T851 (L & T)	2124-T851	5083
5251-H22	5251-H22 (L & T)	6061-T6511	6063-T6
6082-T6	7049-T73	7050-T74	7050-T7451
7050-T7651	7075-T735	7075-T7351	7175-T74
AlMg5Si2Mn Cast	AlSi9Cu3 Cast	AlSi9Cu3Fe Cast	C355 Cast
LM27 Cast	LM27M Cast	LM27TF Cast	
Magnesium Alloys	MgAl2Mn	MgAl4Mn	
AZ91D	MgAl5Mn	MgAl6Mn	
Titanium Alloys	Ti6Al4V (bar)	Ti6Al4V (sheet)	
Bronze	Aluminium Bronze Def Std D833	CW451K Phosphor Bronze	AMS4625G Phosphor Bronze

Table 1: A sample of materials tested by the AMCT laboratory and included in the nCode Premium Materials Database

5.2.2 Static Strength and Cumulative Fatigue prediction tool development for CFRP Composites

For appropriate applications carbon fibre reinforced polymer (CFRP) composites offer many advantages to a designer compared with traditional metal alloy materials. For aerospace the principal advantage is increased strength and stiffness with reduced mass.

However to take full advantage of this benefit requires the ability to optimise structural performance using computer aided engineering (CAE) tools. These CAE tools use finite element modelling (FEM) and finite element analysis (FEA) methods to model the composite structure to predict stress within the structure for a given load condition. Optimising the structural performance uses these stresses from many load conditions to evaluate the capacity of the composite structure to withstand static and fatigue in-service loads.

To evaluate the static strength and cumulative fatigue damage of composite structures subject to complex in-service loads from finite element simulations requires:

- Understanding composite failure modes

- Static strength and cyclic fatigue material data
- To calculate stress in the composite structure [b]
- To evaluate stress against static strength failure criteria
- To calculate stress changes for complex in-service loading histories
- To calculate cumulative fatigue damage and evaluate against fatigue failure criteria

This article considers the development of physical tests to obtain static strength and fatigue material data, and the calculation and evaluation of stress from complex in-service loading histories against static strength and fatigue failure criteria.

[b] This article does not consider the FEM and FEA requirements to appropriately model a composite structure and calculate accurate stresses. There are modelling guidelines and finite element analysis packages that can be used for this.

This article summarises information from References [1], [2] and [3]

5.2.3 Composite Failure Modes

Fatigue is a damage process that can apply to many different materials, but the key feature of fatigue is that it is driven by time varying loads that are smaller than the static strength when manufactured.

Fatigue damage accumulates, the strength and stiffness deteriorates until failure occurs, either because the strength becomes less than the applied loads, or for other reasons – e.g. leaking or unacceptable loss of stiffness.

Failure of a composite is often difficult to define; Is it separation?, Is it cracking?, Is it loss of stiffness or strength?

For composite materials, the failure mode is progressive, from a micro level to a macro level:

- At the micro level - fibre fracture, fibre buckling, fibre splitting, fibre pull out, fibre/matrix debonding, matrix cracking (see examples in Figure 1)
- At the macro (laminate) level - fibre dominated failure, matrix dominated failure, delamination

Failure at the micro scale does not necessarily lead to immediate failure of a laminate, and usually two or more of these failure modes occur in combination. Failure is difficult to detect because it usually originates inside the component and not at the surface.

Failures at the micro-scale will initiate a failure mode but usually plenty of residual life remains. Failures at the macro-level occur at ply drop-offs, edges, defects and impact damage sites.

Fibre failure is the most catastrophic mechanism as the fibres are the primary load-carrier. Matrix failure is the coalescence if micro cracks in the matrix. Delamination is the separation of the ply layers.

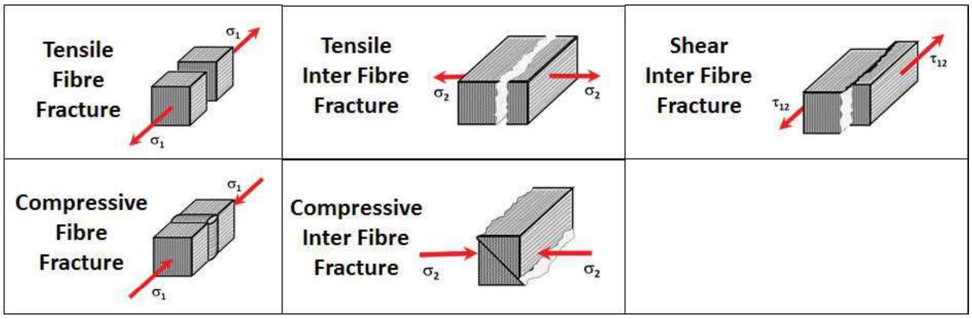

Figure 1 Composite Failure Modes

5.2.4 Static Strength and Cyclic Fatigue Material Data

For a test laboratory with many years' experience testing metal specimens in static and fatigue loading there are many new challenges when developing similar capability for long fibre composite specimens.

These challenges include specialist grips to hold the specimens, anti-buckling guides and finding suppliers capable of manufacturing test specimens from which consistent test results can be obtained.

A successful test specimen failure requires the specimen to fail within the gauge length, and not inside the gripped region or at a grip boundary. Figures 2 and 3 show examples of successful and unsuccessful test specimen failures.

Figure 2: Successful test specimen failures, within the gauge length

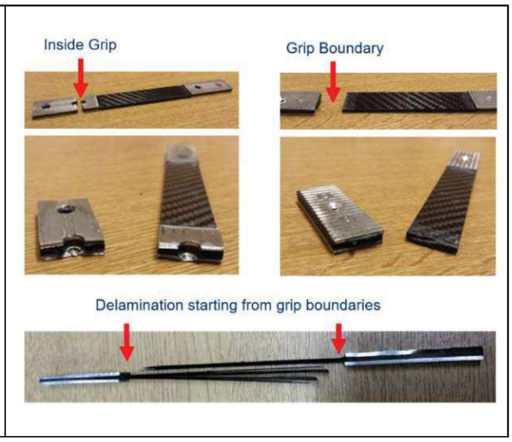

Figure 3: Unsuccessful test specimen failures, within the gripped region, and at the grip boundary

5.2.5 Static Strength Failure Criteria

For metals a common static strength failure criteria is when stress exceeds the material yield stress. Such a yield failure criteria indicates the end of linear elastic behaviour. For metals these yield failure criteria are well known, for example Von Mises and Tresca yield criteria.

For composites there are similar, but less well known failure criteria, for example Hoffman, Tsai-Hill, Tsai-Wu and Franklin-Marin.

Figures 4 and 5, from References 4 and 5, show examples of failure criteria as "failure envelopes" for metals and composites with experimental test results superimposed.

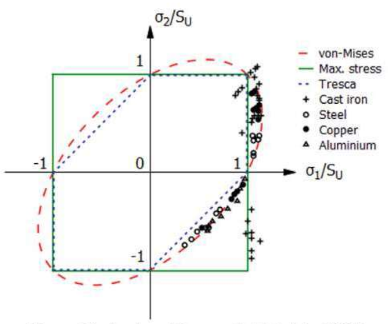

[Jones, Mechanics of Composite Materials, 1999]

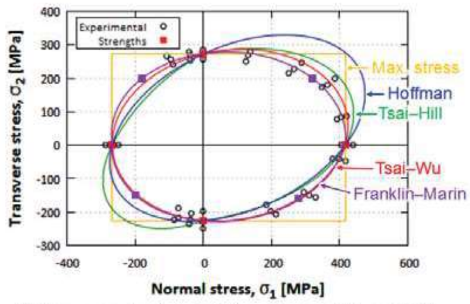

Satin-weave glass/epoxy failure envelope (Tang, 1989)

Figure 4: Yield failure criteria for metals [Ref 4]

Figure 5: Failure criteria for composites [Ref 5]

Figure 6 demonstrates how failure criteria can be shown graphically as a failure envelope. Composite material properties are usually anisotropic in an x-y-z coordinate system with different strengths in the x-y-z directions and different in tension and compression. For long fibre CFRP composites this anisotropy becomes orthotropic in the material coordinate fibre axis, with material properties in two perpendicular directions (σ_1 and σ_2) and in tension and compression.

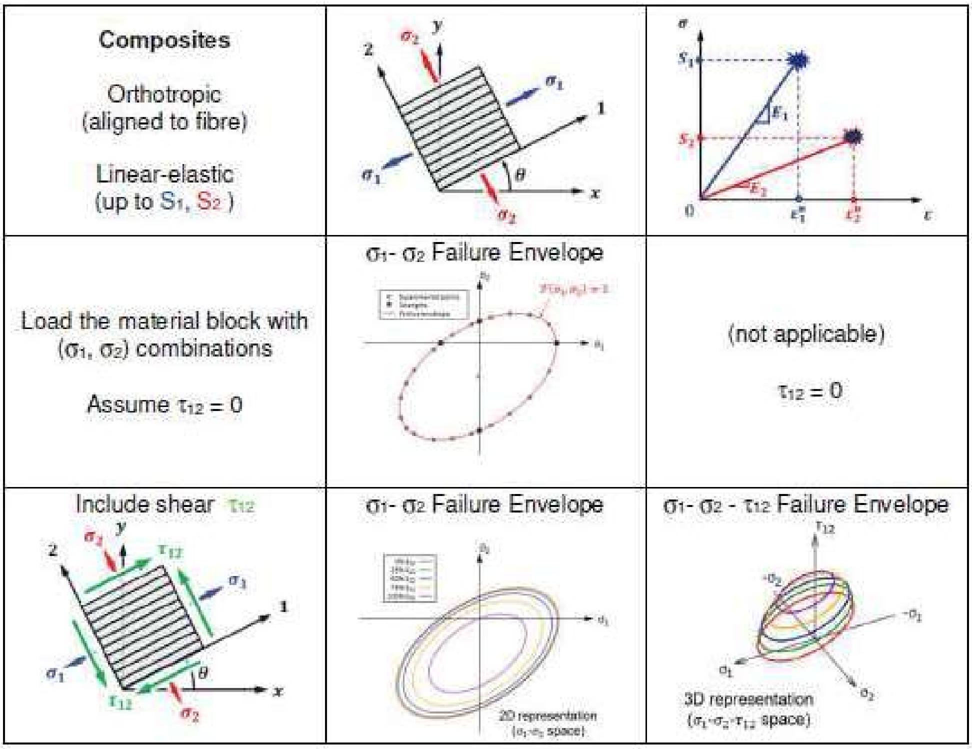

Figure 6 : How a failure criteria can be shown graphically as 2D and 3D failure envelopes

As the material block is loaded with different combinations of σ_1 and σ_2 the failure criteria describes the failure envelope. Where the failure envelope crosses the σ_1 and σ_2 axes gives the strengths σ_1 in tension and compression, and σ_2 in tension and compression.

When a shear stress τ_{12} is included these failure envelopes can be displayed as contours of a 2D plot, or as a 3rd axis of a 3D plot.

5.2.6 Assess Static Strength Failure Criteria from Complex In-Service Loading Histories

FEA is used to calculate the ‘unit load case’ linear-elastic stress response for tension and compression for each loading direction. The in-service loading time history is used to scale these unit load cases and superimpose them for all loading directions.

The result of this is a linear-elastic stress response at every node, in the material coordinate fibre axis, with the perpendicular stresses σ_1 and σ_2, and shear stress τ_{12} (shown in Figure 7).

The failure criteria and the composite material strength properties determines the failure envelope, shown as a cloud of data points, and the resulting load path at a node for a given load history can be combined (shown in Figure 8).

This combined cloud of failure envelope and load path data points can be reduced to parameters that summarise the static strength failure criteria at the node:

- Failure Index (FI) the direct value of the failure criteria function
- Strength / Stress Ratio (SR) a local measure of the margin to failure
- Stress Exposure Factor (SEF) a local measure of the risk of failure (= 1 / SR)
- Margin of Safety (MoS) a local measure of the margin to failure (= SR – 1)

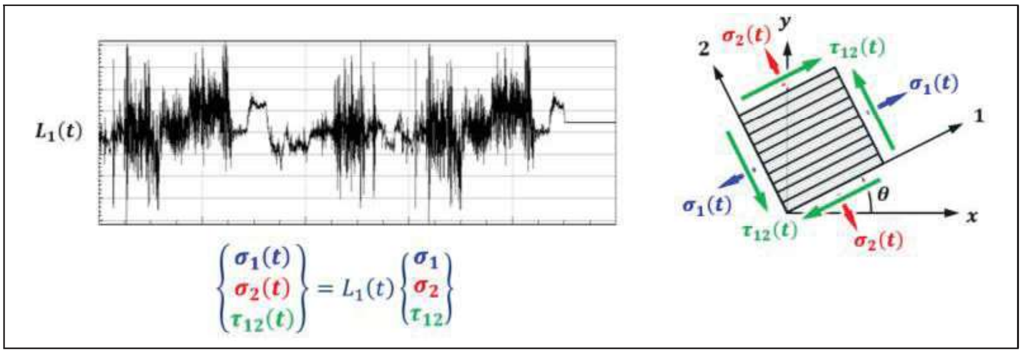

Figure 7 : Perpendicular stresses *□1 and □2, and shear stress*

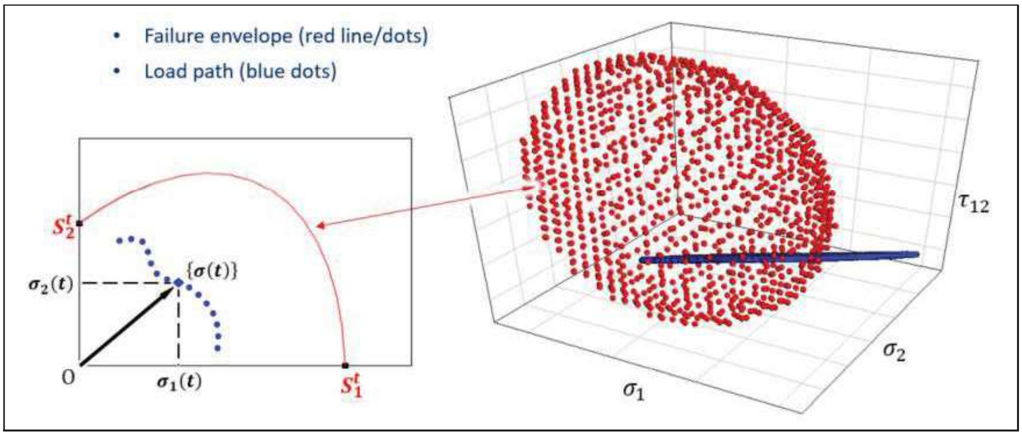

Figure 8 : Failure envelope 'cloud' and load path for a load history

5.2.7 Fatigue Failure Criteria

This considers extending the static failure criteria to account for fatigue. The static strength coefficients are effectively replaced by Haigh diagrams. The Haigh diagram is built from stress-life (SN) curves at different R-ratios, including the critical R-ratio defined by the ratio of the compressive and tensile strengths.

Figures 9 and 10 show an example dataset for a long fibre material comprising 9 stress-life curves at three R-ratios. One curve is shown for each of the three stress components σ_1, σ_2, and τ_{12} (S1, S2 and S12). These figures show the same data plotted in different ways.

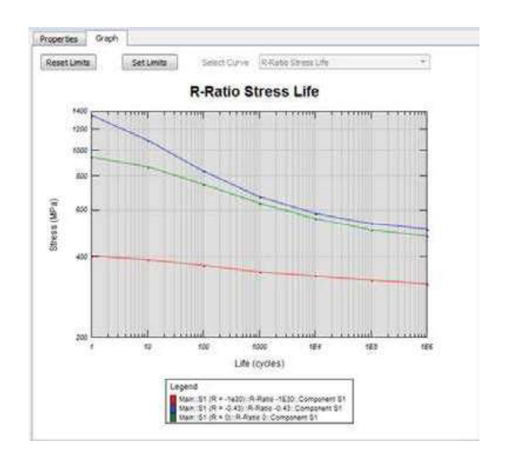

Figure 9 : Example SN curves at R-ratios

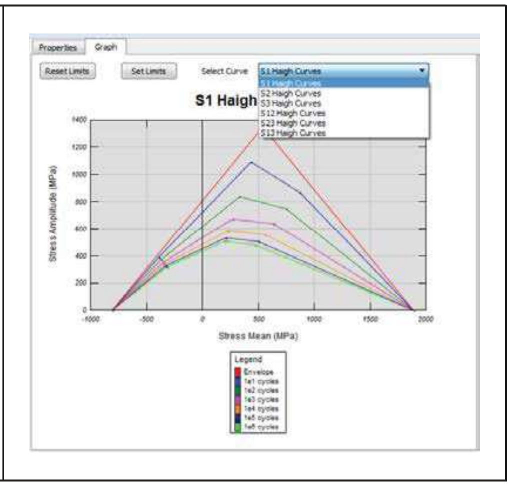

Figure 10 : Example Haigh diagrams

[1] nCode DesignLife Fatigue Theory Manual.

[2] “Strength Prediction of CFRP Composite Structures using the Finite Element Method”, Dr. Peter Heyes and Dr. Andrew Halfpenny, FESI workshop. “Structural Integrity Challenges in CFRP Composites”, www.ncode.com/fesi-composites .

[3] “Fatigue Testing CFRP Composite Specimens”, Peter Lavell, FESI workshop “Structural Integrity Challenges in CFRP Composites”, www.ncode.com/fesi-composites .

[4] Jones RM. Mechanics of Composite Materials, 2nd Ed., 1999 (p.104).

[5] Satin-weave glass/epoxy failure envelope (Tang, 1989).

5.3 BEASY Crack growth software developments

S. Mellings, C M BEASY

5.3.1 Spatially varying sustained crack growth

BEASY undertook a development project to allow the use of variable crack growth rates related to stress corrosion cracking of a structure incorporating welds. Within this structure, specific areas are resistant to crack growth whilst others allow stress corrosion cracking. In addition, non-linear stresses from the welding process will also affect the stress intensity factors.

This development allows these features to be combined with the weld stresses being incorporated in the stress intensity factor calculation and variable crack growth laws applied through the weld structure. This combined behaviour can generate a significant change in the crack growth path, thereby affecting the resulting fatigue life of the part.

The effect of the spatially varying crack growth rate is shown in

Figure for the growth of a simple edge crack through two material regions.

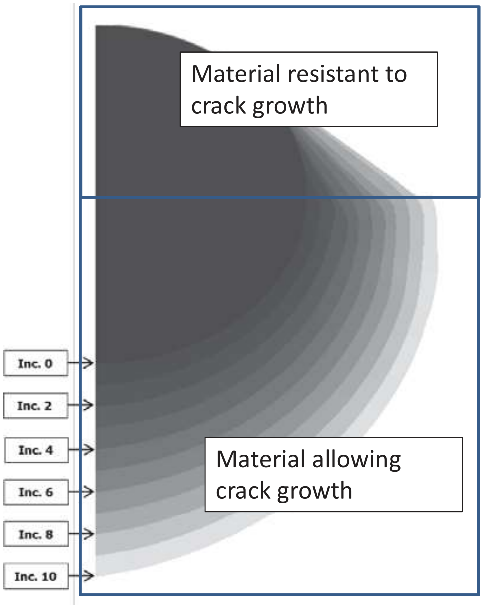

Figure 1: Effect of spatially varying crack growth rate

5.3.2 New flight block based load spectrum file

A further development has been the introduction of a load sequencing file. Under multi-axial loading, it is not always possible to pre-define the fatigue load cycle as applied to a cracked structure. It may be necessary to know the stress intensity factors in order to determine the fatigue cycle. Furthermore, it is possible that under the same applied load sequence, cracks in different locations in a structure (or even at different locations along the crack front) could experience different fatigue loading cycles.

To address these issues, work has been carried out to develop a new loading format in which a series of flight blocks is applied to the model. Each flight block is defined as a sequence of transitions between different load states. In this format of load spectrum file, the load cycling is not pre-defined; rather it is computed at each point along the crack front during the simulation.

This form of analysis computes the crack growth rate in terms of applied flight blocks.

5.3.3 Improved BEASY remeshing

When undertaking a crack growth simulation with BEASY, remeshing is performed at every step of the crack growth process – when either a new crack, or a grown crack, is incorporated into the model.

During 2016 a new release of BEASY introduced a major change in the remeshing tools used within the automatic crack growth process.

New tools were introduced that perform much quicker remeshing and also further improves the mesh quality. This enhancement is particularly relevant to the crack front where the mesh is now continuous and crack front element shapes are optimised. For complex crack front profiles (from the initial or grown cracks) this modification delivers increased accuracy for calculation of the SIF results, and improved crack growth stability. For an example of a particular complex crack front profile addressed by this development see

Figure 2 below.

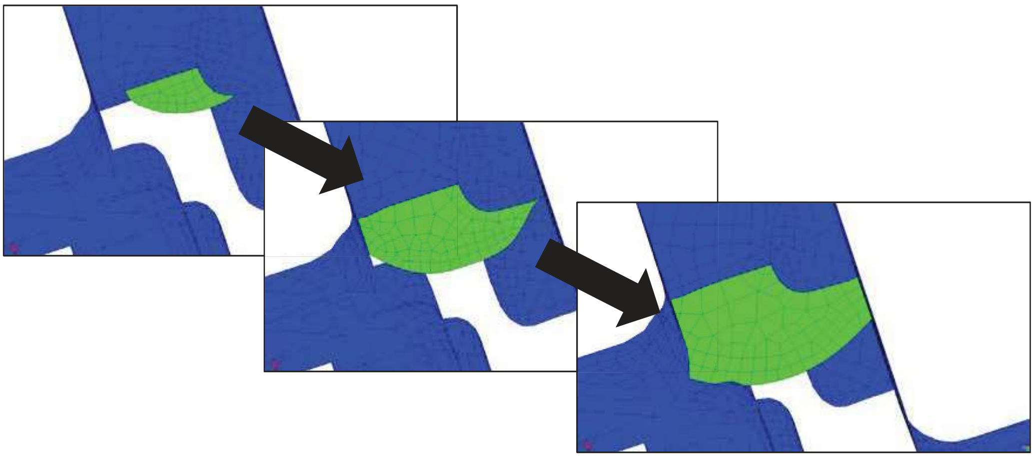

Figure 2: Meshes during steps of crack growth through complex geometry

This improvement can also be seen for simulations where cracks are grown under residual stress loads, around complex external features, and where crack growth is arrested along part of the crack front as shown in Figure 3

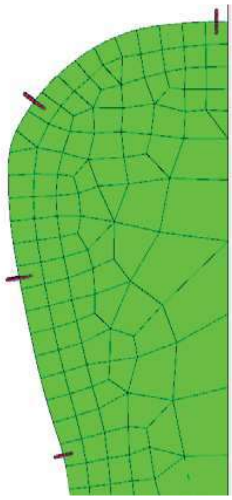

Figure 3: Improved remeshing for partial crack growth case

The development also enables more solutions of models to be obtained on a fully automatic basis (reduced user time).

5.3.4 Improved interfacing with FE models

BEASY simulation allows existing customer FE models to be exploited. Extensive development work was undertaken to further enhance the connections between such models and BEASY, allowing practical use of much larger FE models. The re-designed BEASY-FE interfaces considerably improve the speed of the model generation processes, as well as reducing the time required for residual stress simulations (which interface to the FE models at each growth step).

5.3.5 Reduced solver time

Further development work has also resulted in significant reductions in the computational effort on (parallel computers) for computing the SIF values in a cracked model, specifically for the matrix assembly and the computation of the internal results. This latter calculation is used to compute the J-Integral results, enabling practical use of many more SIF calculation points. This allows understanding of the variation of the SIF values along a crack front, as seen with the stress variation at the ends of the crack in Figure 4. This is the plot of the K1 SIF value along a pressure loaded thumbnail crack at 15 degrees to an external surface.

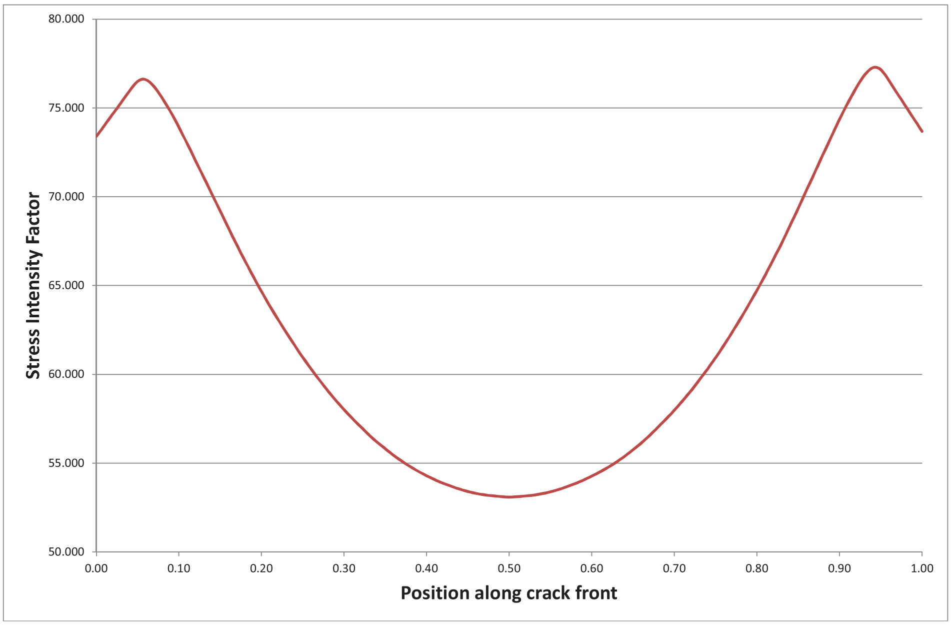

Figure 4: Variation of SIF along the crack front

6 Non-destructive evaluation

6.1 Progress towards the optimisation of ultrasonic phased array parameters for 3D characterisation of aerospace composites

D. Hallam[1,2], M. Mienczakowski[2], [1]Defence Science and Technology Laboratory [2]University of Bristol

Advancements in non-destructive 3D characterisation methods are required to both provide confidence in the quality of manufactured composites components and help underpin the development of optimised aerospace composites designs. To achieve this, there is a need to maximise response from the composite structure to locate and map over a wide area the individual plies and associated defects, such as out-of-plane wrinkling. This work therefore aims to identify the optimum phased array ultrasonic testing (PAUT) parameters for 3D characterisation of aerospace composites based upon the ability to reveal individual plies. A numerical model has been developed with results compared to experimental PAUT data processed using an angle dependant Total Focussing Method (TFM) algorithm and comparative results for a single crystal transducer.

A 6mm thick carbon fibre reinforced plastic (CFRP) composite specimen consisting of intermediate modulus fibres (IM7) within a resin (8552) matrix was manufactured and selected for this investigated due to its widespread use throughout the aerospace industry as double plies of 0.125mm thickness.

A parametric study was undertaken varying the following parameters; transducer frequency (2.5, 5, 10 MHz), number of elements (64, 128), array pitch (0.3, 0.5, 0.63mm), pixel size (0.0025, 0.005, 0.01, 0.02, 0.05, 0.1, 0.15, 0.2mm) and TFM angle limit (off, 10, 20, 30, 40, 50, 60°). Models of four transducers were used; Imasonic 1D 64els 2.5MHz 0.50mm pitch.mat , Imasonic 1D 128els 5MHz 0.30mm pitch.mat, Imasonic 1D 64els 5MHz 0.63mm pitch.mat and Imasonic 1D 128els 10MHz 0.30mm pitch.mat . An analytical full matrix capture (FMC) model was developed in Matlab and for each transducer specification, the FMC data output files were imported into the Bristol Array Imaging (BRAIN) software for post processing visualisation. As an example, figure 1 presents a series of b-scan images from a 5MHz 128els 0.30mm transducer arranged in decreasing pixel size.

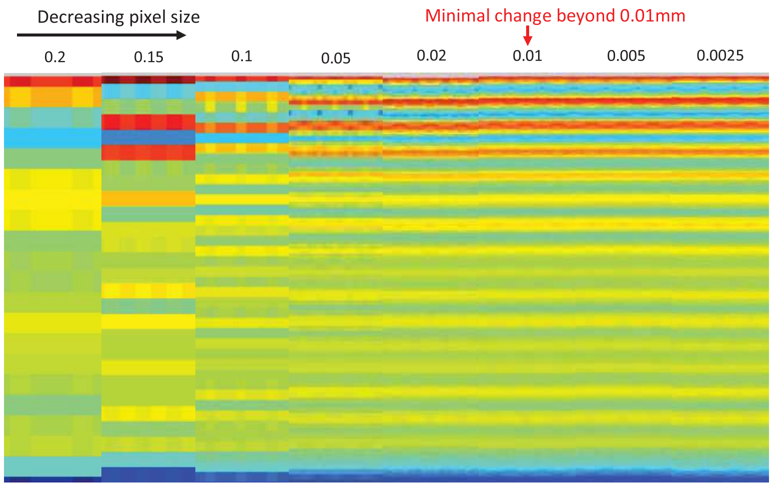

Figure 1: A series of b-scan images comparing pixel size (0.2 – 0.0025 mm) for a 5MHz 128els 0.30mm transducer. All images are taken from the same location within the sample.

Qualitative assessment reveals that the optimum set of PAUT transducer and TFM parameter values for the inspection of plies in an IM7/8552 composite sample appear to be from using a 5MHz 64els 0.30mm transducer with a pixel size of 0.01mm and an angle limit of 30°. In an effort to quantify the ability to reveal individual plies, signal to noise (SNR) ratios for each transducer and parameter combinations were also determined from the frequency response. An example is shown in Figure 2.

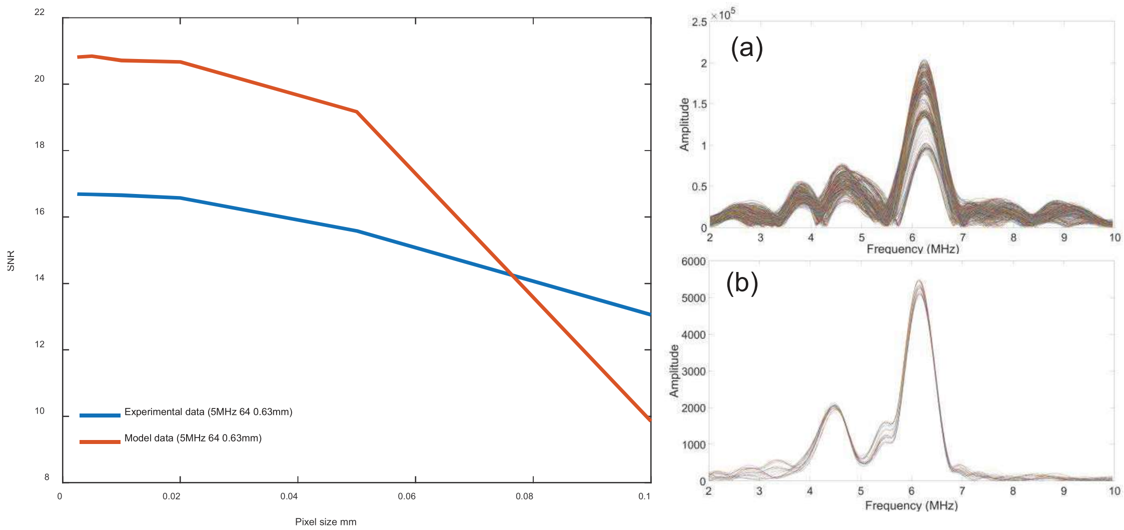

Figure 2: The variation in SNR with decreasing pixel size for a 5MHz 64 element 0.3 mm pitch spacing modelled transducer, plateauing at a pixel size between 0.01-0.02mm. The corresponding amplitude-frequency graphs for (a) experimental and (b) modelling data at a 0.01 pixel size, revealing a ply resonance of approximately 6MHz is also shown (inset).

Using the optimised TFM parameters as determined from the parametric modelling study, a comparative PAUT experimental study using identical transducers parameters was conducted. A direct comparison between modelled and experimental data for a 5MHz 64els 0.63mm transducer is shown in figure 3. This is accompanied by comparable data obtained using a 5MHz single crystal transducer in immersion, all of which show relatively close agreement in their ply locations. Future work aims to continue to quantify the signal to noise ratio of the other variables (model and experimental) to identify an optimised set of parameters to enable wide area 3D characterisation of aerospace composites.

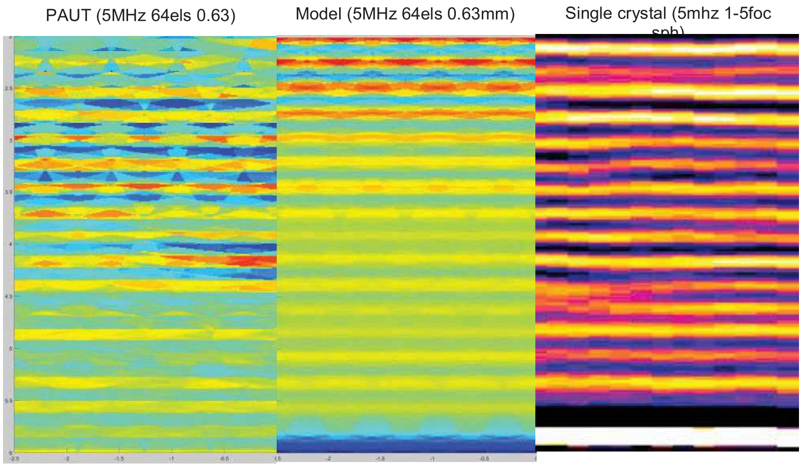

Figure 3: Three b-scan images directly comparing experimental PAUT, modelled and single crystal data at the same transducer frequency (5MHz).

The authors would like to acknowledge the EPSRC Industrial Fellowship of Professor Robert Smith and Dr Ollie Nixon-Pearson for the manufacture of the composite sample. The prior work developing the analytical model undertaken by Yosef Humeida, the single crystal NDT data acquired by Annabel Dance is also gratefully appreciated.

6.2 Model Assisted Qualification of Non-Destructive Testing Inspections

A Ballisat, University of Bristol

The time consuming and expensive nature of Non-Destructive Testing (NDT) inspection qualification hinders the introduction of techniques into service. The use of numerical models, such as finite element simulations, has the potential to replace a significant proportion of the empirical trials that are typically performed to demonstrate the capability of a technique. This has become more feasible in the last decade with the significant increase in computational power available, especially the advent of parallelised calculation using graphical processing units (GPUs). This project aims to develop a methodology that minimises the number of simulations that have to be performed in order to demonstrate the capability of a technique.

A key feature of this approach is to note that many inspections result in single valued scalar quantities, such as an amplitude, phase or an area on an image. It is therefore possible to sample the parameters that vary in the inspection, simulate the resulting variability in the response and from this infer through interpolation every possible response of the inspection. Coupling this with the probability of these variations occurring allows metrics such as the Probability of Detection (PoD) and Probability of False Alarm (PFA) to be calculated, giving a quantitative measure of the capability of the technique. Crucially, no assumptions are made as to the nature of the response and non-linearity, discontinuities and interaction between different parameters could all potentially be present. The effect of parameters on the outcome of the inspection can be calculated using a sensitivity index which provides a quantitative measure of the variance in the outcome of an inspection that can be attributed to each parameter and the interactions between them.

This methodology also provides optimisation as a by-product as all points in the parameter space are desired thus optimisation is simply picking out the single best point. Furthermore, the quantitative measure of the importance of parameters provides insight into which parts of performing an inspection need to be paid most attention by an operator, thus providing further benefit when designing and qualifying a technique.

The following describes the application of these methods to a simple example inspection of a single element probe ultrasound inspection of a crack emanating from a bolt hole in an aluminium wing skin, as shown in Fig. 1. Three parameters are allowed to vary: the probe's lateral position, x, perpendicular position, y, and the rotation of the probe on the surface of the sample, θ. This was modelled in Pogo FE in 3D with each simulation taking approximately 8 minutes on a powerful desktop PC. The predictive interpolation error is shown in Fig. 2. This demonstrates that it is possible to sample and interpolate the parameter space to within a low predictive error in a small number of simulations. For brevity, the PoD curves are not shown here however can be easily calculated for any of the parameters considered. The sensitivity of the inspection to the different parameters, and the interaction between them is shown in Fig. 3. This shows that the angle of the probe is the most important parameter and that there is strong interaction between several parameters however only weak interaction between the x and y positions. This suggests that the operator should pay most attention to rotating the probe to maximise the response whilst not being so concerned with how far … they are.

Current work is experimentally validating this methodology on specimens of the above inspection before moving onto applying it to an in-service inspection.

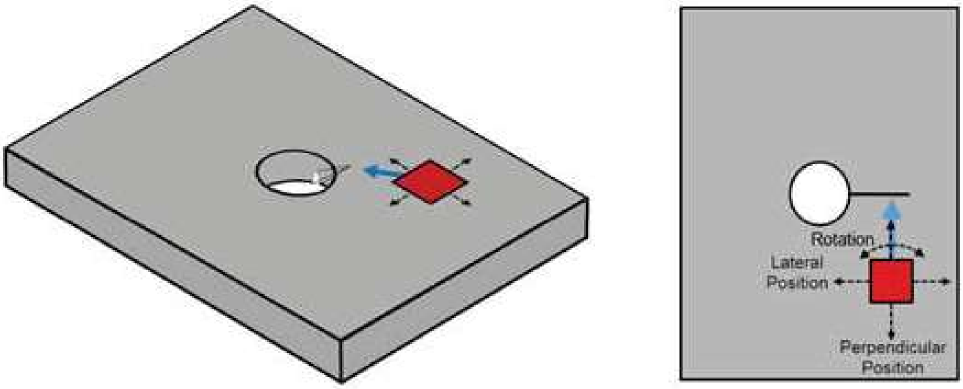

Figure 1: Schematic diagrams of the inspection investigated from a fastener hole: (a) isometric and (b) plan view.

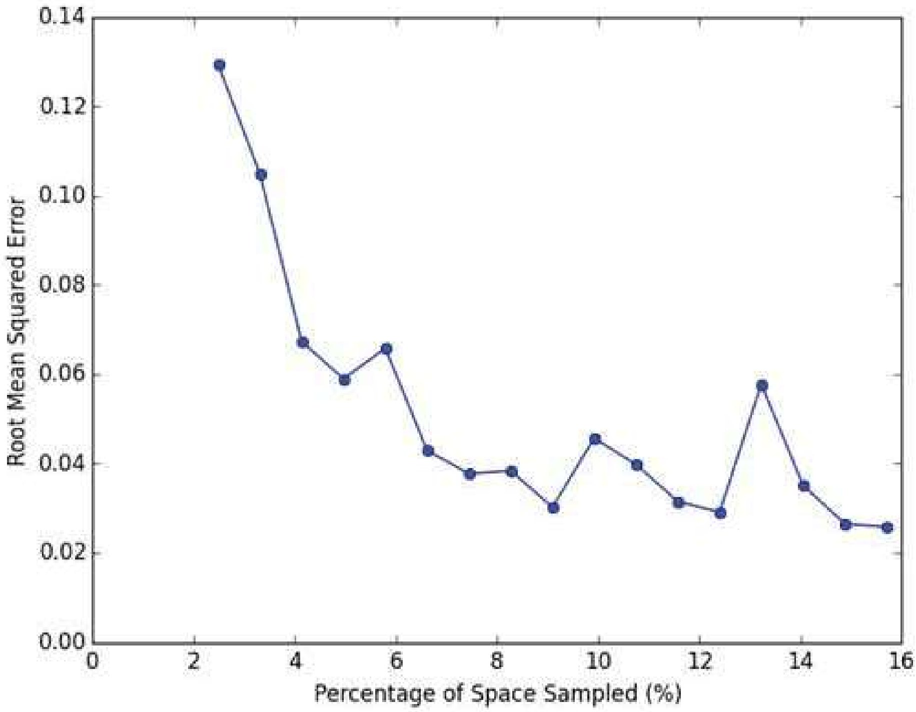

Figure 2: The predictive error of the sampling and interpolation as a function of the percentage of the parameter space mapped. All responses are normalised thus the error plotted is the normalized error.

ANNEX A

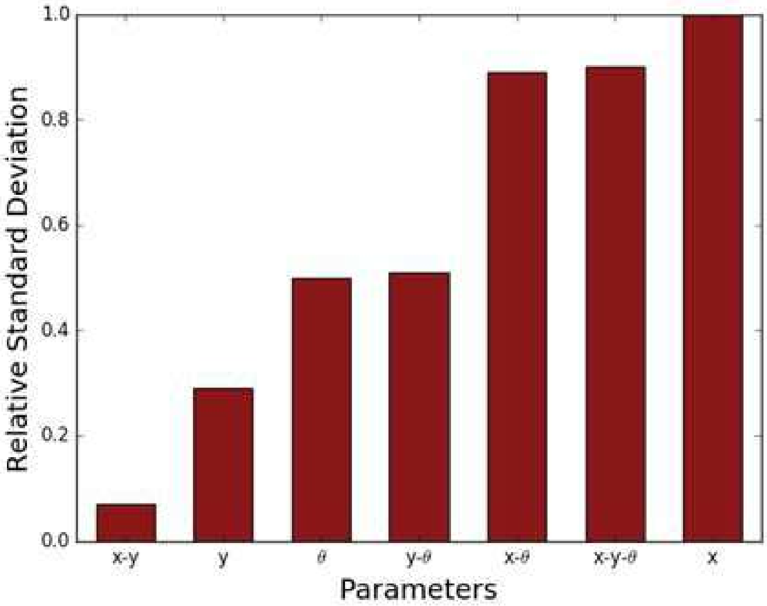

Figure 3: The relative importance of parameters and their interactions measured by their contribution to the total standard deviation of the response.

6.3 Introduction of new non-destructive testing capability

D. Hallam, Defence Science and Technology Laboratory (Dstl)

Despite Non-Destructive Testing (NDT) being one of the primary tools required to support the continuing airworthiness of aircraft structures and systems, there are significant impediments to the introduction of new NDT capabilities into service.

A proposal to address the main issues, by developing a Model Assisted Probability of Detection (MAPOD) approach, was proposed by Professor Robert Smith, Professor of NDT and High-Value manufacturing at Bristol University. His proposal, Paper 122, was endorsed by the Military Aviation Authority-Chaired 77th Military Aircraft Structural Airworthiness Advisory Group (MASAAG) and this approach is supported by the British Institute of NDT (BINDT). This paper is now published on the UK Government Website, www.gov.uk, under MASAAG Papers.

A combined academic and industrial programme, involving TWI Ltd and the University of Bristol, to meet the agreed MAPOD approach has been developed. An Engineering Doctorate (EngD) programme is underway, considering the modelling aspects of this problem. In parallel, the contract to develop and demonstrate the MAPOD protocol for the introduction of new NDT capabilities has now been let, following a competition, and progress on this task will be covered in future summary reports.

The programme to create, draft and demonstrate a protocol for model-assisted NDT technique validation was awarded to TWI and commenced in May 2016. The first deliverable, a literature review, was received in October 2016. This was followed by the first Industrial Advisory Group (IAG) meeting held in January 2017, attended by a wide variety of key industrial organisations (including MOD, Rolls-Royce and Airbus). Industry partners have agreed to provide access to existing procedures, data and test reports and test sample identified as being ideal to test the protocol being developed. Wider publicity of the work is being made through regular involvement with the British Institute of NDT (BINDT) and the European- American workshop on reliability of NDE.

7 Corrosion protection and prevention

7.1 Understanding the corrosion threat to military ageing aircraft

Dennis Taylor, Dennis Taylor Associates Ltd

With many military aircraft platforms being required to operate past their original out of service date (OSD) there is an increasing concern that structures and systems may be experiencing an increased airworthiness risk from corrosion. Therefore, a corrosion survey, across all the air platforms looking at arisings and best practice solutions has been undertaken by Dennis Taylor Associates. The findings, with key recommendations for remedial actions and identification of beneficial practice have been reported as Ageing Aircraft Working Group (AAPWG) Paper 012 [1]. Paper 012 has been subject to industry and MOD peer review and has been published on the UK Government Website (www.gov.uk), under AAPWG Papers. Implementation of key recommendations is underway in MOD Air Fleets.

[1] Taylor, D., Understanding the Corrosion Threat to Ageing Aircraft, Ageing Aircraft Programme Working Group (AAPWG) Paper 012, Final, December 2015.

7.2 Coating Degradation and Corrosion Sensing

A. Cafearo, R. Eley, C. Figgures, I. Sturland and M. Balmond, BAE SYSTEMS Advanced Technology Centre

7.2.1 Paint Coating Degradation (PCD) Sensors

The Paint Coating Degradation (PCD) sensor (Figure 1) monitors paint coating degradation continually and provides an early warning of corrosion before it becomes an expensive problem. The sensor output changes when the paint's corrosion inhibitor system is no longer able to protect the alloy that is exposed by the engineered defects in the coating. The engineered defects are 3 slots with different widths in order to provide a graded measure of inhibitor degradation over time. The sensor was developed due to the cost of corrosion to the defence industry, which is estimated to be more than 40 billion dollars per year in the USA alone and is estimated to be a similar percentage of GDP in the UK and in Australia.

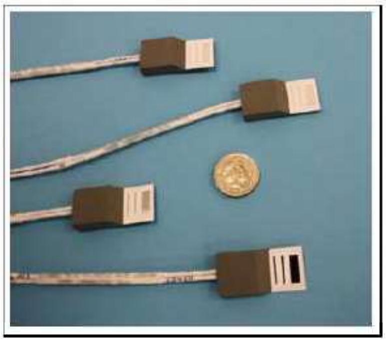

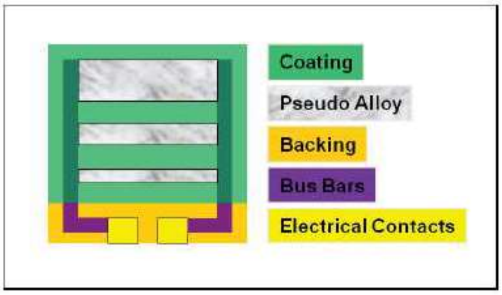

Figure 1: PCD sensor and schematic

The sensors are referred to as Smart Witness Plates because they are made in the same way as the bulk material witness plates that are used to test the effectiveness of paint coatings in various environments. The difference is that the smart sensor provides an electrical output which changes as the material corrodes due to degradation of the paint scheme, whereas conventional witness plates have to be taken back to the lab for analysis under a microscope. These sensors can be installed on platforms in areas that are difficult to access – in sealed bays/compartments, behind equipment etc.

Sensors have been tested alongside conventional bulk material witness plates during characterisation trials in an outdoor environment, illustrated in Figure 2.

Figure 2: PCD testing alongside bulk material witness plates

In addition to trials on aircraft/ships/vehicles and trials in outdoor environments, sensors have been put through accelerated testing alongside conventional bulk material witness plates in the laboratory in order to characterise sensor performance

Figure 2: PCD accelerated testing alongside bulk material witness plates

7.2.2 Development to date

The sensor operation has been proved by outdoor characterisation testing and accelerated testing in the laboratory. The sensors have been developed with both 2000 and 7000 series Aluminium alloy sensing elements and with both chrome and chrome-free primer coatings.

It is a significant challenge to adequately protect the electrical interconnections to sensors in harsh corrosive environments for long periods of time, when the sensing elements themselves need to be fully exposed to the environment (meaning that total encapsulation of the device is not an option). A novel sensor packaging technique has been developed to replace the method that was used for original prototypes in order to make units that are robust enough for long term use in such harsh environments.

Sensors manufactured using the new packaging process have survived long term immersion testing in salt solution and temperature cycling over the full Mil Spec temperature range. The process has also been productionised in order that it is suitable for volume manufacture.

PCD sensors are currently fitted to every F-35 aircraft that is produced and the outputs from all sensors are monitored remotely through the Autonomic Logistics Information System for development purposes. There is now an intention to begin fitting the latest robustly packaged sensor variant to enable through-life use of the technology on this platform.

Trials have been carried out on Typhoon, Tornado, Hawk, Sentry, Ships and Land Vehicles with a view to developing sensor variants & data logging systems appropriate for use with sensors when retro-fitted to platforms that do not have existing ports available for the connection of corrosion sensors.

7.2.3 Summary

The PCD sensor can monitor paint coating degradation continually and can provide an early warning of corrosion.

Areas that are difficult to access can be monitored without the need to open up the bay/compartment to carry out inspections.

The sensors are very sensitive and provide alerts when corrosion pits begin to form that are only 30 microns in diameter (far earlier than they can be seen by the human eye). Knowing about corrosion events this early means that the issue can be dealt with before it becomes serious.

One of the biggest costs of corrosion is the cost of inspections. By using sensors to monitor continuously and avoiding the need to access all locations on such a frequent basis, big savings can be made on inspection costs.

Data from sensors on all aircraft in a fleet can be fed back to a central engineering support system and the status of sensors is displayed in a simple traffic-light format i.e. the amber condition is an early warning that does not need to be acted upon immediately and allows planning of appropriate maintenance activities in advance (before a red light condition occurs), as illustrated in Figure 3.

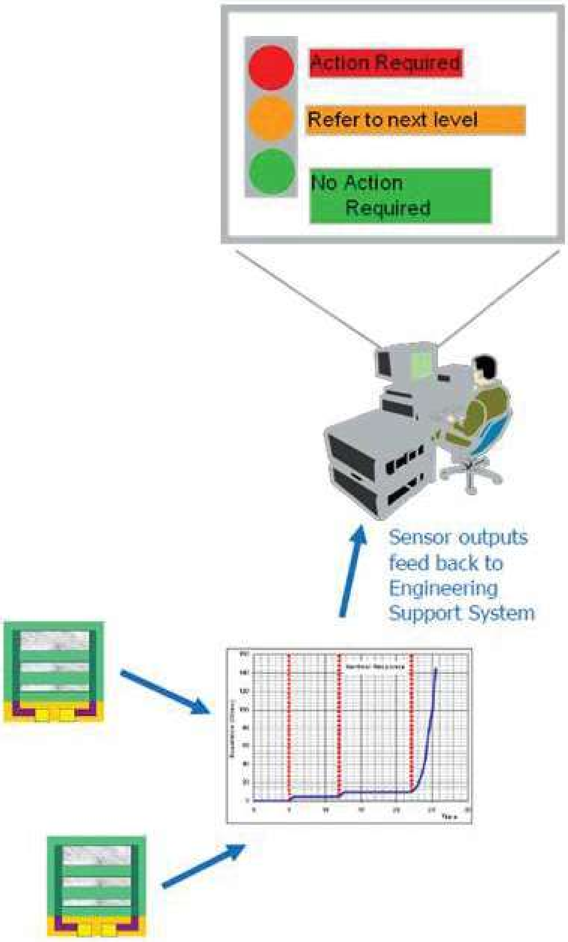

Figure 3: PCD operations schematic

7.3 Dehumidification of UK military aircraft

D. Moody and R. James, Musketeer Solutions

The positive effects obtained from the use of dehumidification (DH) on parked aircraft, have been well documented over a number of years. Maintaining the Relative Humidity (RH) in the aircraft at around 40% slows significantly the onset of mechanical corrosion, whilst improving considerably the reliability of the aircraft systems by removing moisture from the inside of the avionic ‘black boxes’. Investigations suggested that, whilst the advantages of applying DH were well known, the actual deployment and application DH was not as widespread as perhaps it should have been.

The first step was therefore to understand why there was this reluctance to embrace the DH concept. Further research suggested 3 main reasons:

- The interconnecting equipment is cumbersome and difficult to use - On a large aircraft DH is applied at a number of specific points, requiring a series of heavy hoses to be stretched the length of the airframe

- The DH units are unreliable - Perceived as unreliable, but probably as a result of under utilisation

- Lack of education on why DH needs to be applied continually - The payback of applying DH can only be measured over an extended period of use; no immediate benefits can be seen by those tasked with operating the equipment

In order to establish the credibility of the DH concept, 2 on-aircraft trials of DH equipment were commissioned: a rotary wing and a large fixed wing aircraft were chosen. The latter would normally have DH applied at 3 locations on the aircraft, but for the purpose of this trial, a single point DH application was used. The trials were carried out on two retired aircraft which had been allocated to the MOD Ageing Aircraft R&D Programme and known colloquially as Ageing Aircraft Programme Laboratories (AAPLs).

Figure 1: Puma Ageing Aircraft Programme Laboratory

There was no dedicated point on the Puma aircraft to apply air conditioning or DH. Therefore, an adaptor was manufactured, which fitted into the cockpit window. It should be noted that this aircraft does not have a pressurised hull. Hence, the DH air leaks from the cabin of the aircraft into the fuselage, which equalises the overall RH.

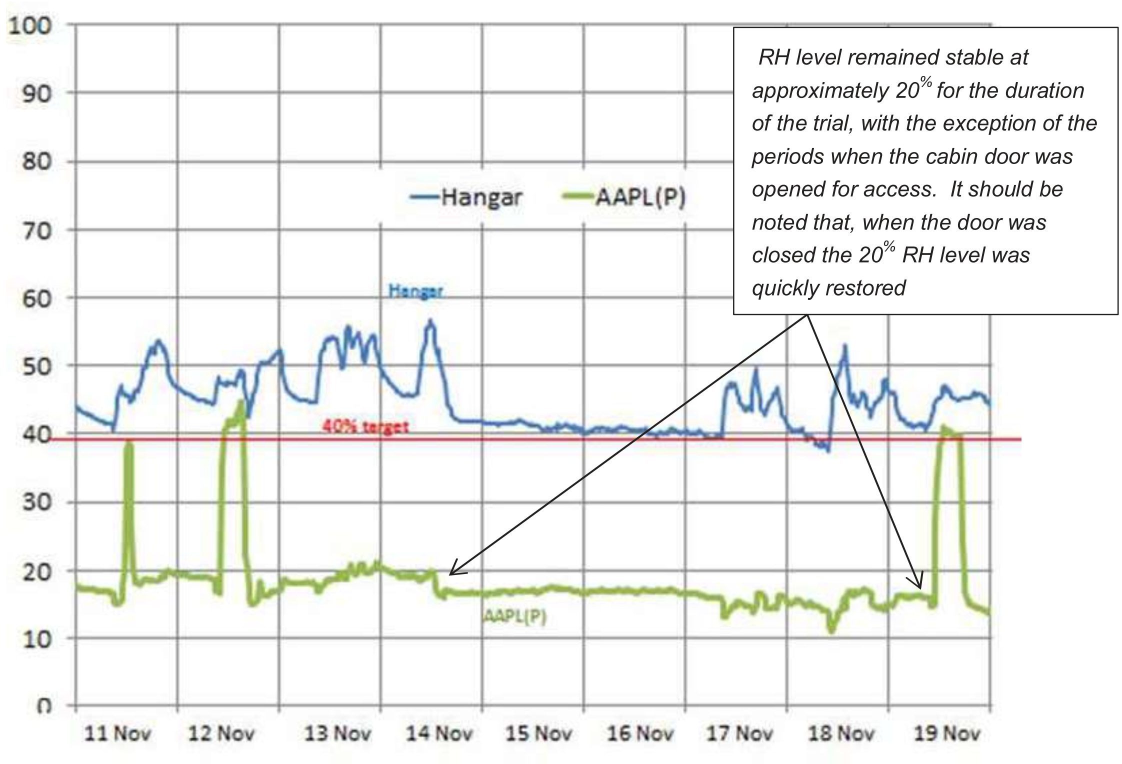

Figure 2: Puma dehumidification trial

The graph in Figure 2 is a snapshot of the results achieved during the period 11 - 19 November. The actual trial ran from 28 October to 6 January and these results are representative of those obtained throughout the trial. The same DH unit was used throughout the trial, without any malfunction. Similar results were recorded on the large fixed wing aircraft.

Following the success of the airframe DH study a further trial has been commissioned to measure the effects (positive or otherwise) of applying DH to installed engines (Figure 3). This trial is scheduled for mid-2017.

Figure 3: Sentry engine DH trial configuration

7.4 Improved landing gear surface finish and repair

Dr Jay Patel, QinetiQ

Numerous in-service issues have been identified of paint damage on undercarriage legs (see Figure 1). Many of the substrate materials are very susceptible to corrosion and could suffer mechanical failure arising from small size damage caused by impacts and subsequent corrosion.

Four coating systems were identified by QinetiQ as having potential to improve the corrosion protection of landing gear. Of these four paint systems, it was found that the PR205/EC94 system provided the best overall performance [1]. Polymeric films (in the form of tapes), with the aim of enhancing the protective functions of the paint films, were also assessed. Two protective tapes were identified with the supplier, 3M, based on the current use such films for the leading edges of wings and rotor blades.

The two candidates, 8542HS and 8641 were applied to the test specimens coated with the successful EC94 paint system mentioned above. Using the similar test procedure as that adopted for testing the paint systems, the 8641 polymeric film was found to perform better than 8542HS.

Substrates considered were 4340 alloy steel, 7075-T6 aluminium and mild steel. The pre-treatments considered were cadmium plating, chromic acid anodising and grit blasting. In all 6 coating candidates tested with and without polymeric tapes. The test regime considered application, fluid resistance, impact resistance, thermal resistance, corrosion resistance and repairability. The laboratory work has been completed and the next phase is aircraft trials of the best performing products

Recommendations have been made to trial the EC94 paint system and the 8641 polymeric film on aircraft. It was also recommended that a Defence Standard would need to be drafted to ensure better performing materials are procured for landing gear systems. These recommendations will be considered, with the relevant authorities, within the ongoing programme.

[1] Patel, J. N., Task AA1430/1 Landing Gear Surface Finish and Repair Best Practice - Final Report, QINETIQ/16/00498/1.0, 17 March 2016.

Figure 1: Example undercarriage surface finish damage

7.5 Corrosion protection – Electrical bonding

D. L. Bartlett, QinetiQ

Surveys of ageing aircraft found corrosion on fuel and hydraulic pipes, and structure at bonding points (see Figure 1). Sealant or corrosion protection compounds (CPC) can trap moisture which increases risk of galvanic/crevice corrosion under bonding straps and makes inspection difficult.

Better coatings are required for corrosion protection and improved inspection regimes. Five candidate coatings have been identified and tested with and without sealants, using test specimens which were bonding straps bolted to plates. Testing considered application, adhesion, vibration and flexibility and the environmental tests included Skydrol, fuel, intermittent and continuous salt spray. The best performing semi-transparent coating recommended for an implementation trial. In addition, recommendations [1] were made for changes to the management of electrical bonding in service.

[1] Bartlett, D. L., Electrical Bonding Straps Corrosion Protection Best Practice, End of Task Report AA1430/2, QINETIQ/15/00510/2.0, November 2015.

Figure 1: Example electrical bonding related corrosion

7.6 Impact of Registration, Evaluation, Authorisation and Restriction of Chemicals (REACH)

J. N. Patel, QinetiQ

7.6.1 Identification of Surface Finish Registration, Evaluation, Authorisation and Restriction of CHemicals (REACH) Issues

The REACH process involves the assessment of registered chemicals; those chemicals that are judged to be candidates for the SVHC list (currently 173) or the restricted list are then placed on the appropriate listing for comments by interested parties, including consortia, who have a vested interest in the chemical. If authorisation is not granted, then the substance/chemical will not be available after its 'sunset' date. This process occurs at approximately six-monthly intervals and the list is therefore expected to increase over time.

The REACH regulations affect the use of a range of products including: paint removers, solvents, conversion coatings, primers and top-coats. All of these products are used for maintenance activities on UK military aircraft.

QinetiQ [18] has identified the new substances that have been added to the Authorisation, Candidate, Restricted and Authorisation, Candidate, Restricted, and Community Rolling Action Plan (CoRAP) listings. As these listings are regularly updated by the European Chemicals Agency (ECHA), this work is expected to continue for the foreseeable future.

The main effort on this task has been the continued development and population of the REACH database with paints, constituents (such as chromates and solvents) and other related products. The database, which is co-sponsored by the DE&S Airworthiness Team, allows a substance to be tracked to a product and to the affected aircraft or project team and back the other way. Hence, the database can be interrogated to identify all of the products at risk for a particular aircraft type.

Maintenance products containing chromate compounds appear to be the most severely affected and account for a large proportion of the SVHCs. These chromate compounds are of importance for corrosion protection of aircraft structures and systems.

The database currently contains data for Air Commodities Surface Finish (ACSF) and 9 aircraft including C-130J, C-17, Chinook, Sentry, Lynx, Merlin, Sea King, Tornado and Typhoon; population with data from other aircraft types is ongoing as is the evolution of the lists of affected consumables.

It is intended that the database will become a common tool used by all relevant agencies for the management of REACH affected surface-finish related products. The possibility exists for the database to be extended to cover products other than those used for surface coatings, for example sealants, and/or non-aerospace applications but this is outside of the scope of the current programme.

7.7 Surface finish lifing methods

J. N. Patel, QinetiQ

The aim of this work programme is to develop non-destructive methods of assessing the integrity and 'life' of surface finish (paints) for systems with primer only and primer and top-coat.

One element of the work focussed upon using laboratory X-Ray Fluorescence (XRF) (see Figure 1) techniques to determining the chromate content of primer paint films. This year the aim was to develop the use of hand-held XRF techniques to allow in-service application. The differences identified in initial comparative results in the Chromium:Titanium (Cr:Ti) ratios (used for life assessment) measured on test panels between the hand-held and laboratory XRF equipment were larger than expected, when compared with laboratory equipment results. This was investigated with the manufacturer (Oxford Instruments) and a modification to their software was produced. On retesting, the instrument was found to produce consistent results suitable for monitoring changes in the Cr:Ti ratio and hence the chromate content [1].

Recommended approaches for determining the chromate content in primers applied to service aircraft have been developed. However, before the XRF spectrometer can be deployed on service aircraft, local safety risks will need to be assessed for the aircraft and working site. This technique is considered most valuable when relative Cr:Ti ratios can be identified and hence baselining a fleet is considered the best approach. This will be considered further in the ongoing programme.

Figure 1: Hand-held XRF machine

In addition, development of an evidence-based approach to lifing of surface finish systems has continued. The aim is to use an on-condition approach (such as the measurement of colour and gloss levels), rather than a fixed-life approach, where appropriate. This work has been undertaken in collaboration with 1710 NAS and the relevant aircraft PTs. This year this approach has been applied to Hawk T1 aircraft and initial assessments Hawk T2 aircraft have been undertaken. Further work is planned for the forthcoming year for Hawk T2 and an initial assessment of Typhoon is proposed (in collaboration with BAE SYSTEMS).

[1] Patel, J. N., Development of XRF Technique Final Report, Task AA1430/12, QINETIQ/16/00666/1.0, 17 March 2016.

7.8 Corrosion protection – hot air ducts

D. Bartlett, QinetiQ

The aim of this task is to identify the most appropriate coatings for hot air ducting. Several instances of corrosion damage to hot (bleed) air ducting have been identified during condition surveys of ageing aircraft (see Figure 1). Corrosion occurred through incidental damage to removable or permanent thermal insulation (cladding) which resulted in severe corrosion of the hot duct surfaces that remained hidden by the cladding.

QinetiQ has identified the materials typically used for hot air ducting (stainless steel operating in the mid to high temperature range (150-300°C)) and has identified four candidate coatings for testing based upon corrosion and insulation properties.

Testing was conducted on sections of welded duct (recovered from the WEST) coated with these products and included thermal resistance, corrosion resistance by intermittent salt spray, cyclic humidity, extreme low temperature, resistance to hot hydraulic fluid and vibration.

QinetiQ concluded [1] that IP9064 barium chloride epoxy-based primer was considered the best option for corrosion protection of hot air ducts reaching temperatures of 200°C. The epoxy- or silicone-epoxy based primers assessed in this programme were not recommended for higher temperature hot air ducts.

[1] Bartlett, D. L., Task AA1430/08 – Corrosion Protection for Hot Air Ducts - End of Task Report, QINETIQ/17/00018/1.0, 20 March 2017.

Figure 1: Example hot-air duct corrosion

8 Structural integrity assurance

8.1 A Framework for Ageing Aircraft Audits

Martin Hepworth, Aviation Support Consultants

The Defence Science and Technology Laboratories (Dstl), with the support of the Military Aviation Authority (MAA) through the Ageing Aircraft Programmes Working Group, have initiated a research and development programme titled “Understanding Ageing Aircraft”. This paper, “A Framework for Ageing Aircraft Audits” contributes to this programme.

The MOD has been carrying out Ageing Aircraft Audits (AAA) for over 15 years initially the audits concerned only the ageing of aircraft structure. However, following the high profile loss of two commercial airliners and perhaps more poignantly the loss of Nimrod XV230 over Afghanistan in 2006, AAA were extended to encompass sub-audits for Systems and Propulsion System. In the intervening period considerable experience has been gathered carrying out AAAs and this paper seeks to expand on selected areas of the current policy laid down in MAA Regulatory Article (RA) 5723. It provides additional guidance and introduces some new suggestions based on best practice from within the MOD and from the wider aviation community. A background is provided to events leading to the current approach to identifying Ageing in Aircraft, both Military and Civilian.

The importance of pre-audit planning is stressed and guidance is provided on the subjects that should be covered in this important phase of the Audit.

The Paper breaks the AAA tasks down into four areas. Experience has shown that there are aspects of the audit that are common to the three sub-audits areas of Structure, Systems and Propulsion System.

RA5723 mandates that the audit include an independent physical examination of representative aircraft, however it does not expressly mandate intrusive forensic sampling. This paper includes details of the types of conditions survey that will satisfy the requirements and provides details of the purpose and management of a condition survey. It also provides an insight into more in depth surveys.

Finally, selection of common forms of material degradation given with a shot description of what an AAA Team should be aware of. The list is not extensive but merely seeks to provide an insight into material ageing.

The Framework for Ageing Aircraft Audits Ageing Aircraft has been endorsed by the MOD/Industry Ageing Aircraft Programme Advisory Group (AAPWG) as Paper 010 and is published on the UK Government Website (www.gov.uk) under AAPWG Papers.

8.2 Structural teardown of a Tornado GR4 aircraft

W. Martin, QinetiQ

Structural sampling or teardown is an invaluable tool in structural integrity assurance. Principally it is used to ensure the in-service maintenance procedures are providing the level of assurance that is expected of them and that there are no unseen issues, particularly ones that cannot be replicated adequately on a full scale fatigue test, that are posing a threat to the structural integrity of the fleet. Typically, this would be focussed primarily on corrosion and mechanical damage but programmes have identified fatigue issues where structure is either not represented on the fatigue test or is not representatively loaded or to identify the occurrence in-service of previously identified fatigue test findings.

QinetiQ has undertaken a teardown examination of a retired Tornado GR4. The selected aircraft, ZA410, was a Tornado GR4 trainer version that first flew on 3 March 1983. ZA410 had accumulated just over 6568 flying hours before it was retired from service and introduced to the Reduce-to-Produce (spares recovery) programme. The findings from the teardown activity have since been fed into the structural integrity programme for the Tornado.

The full extent of the teardown findings for Frame X11185 and X10910 is too extensive to report in this summary. However, an example of the findings is presented here. Figure 1 illustrates fuselage frame X11185 and shows a summary of some of the damage found and the frame location on the aircraft.

Frame X11185 is a machined frame with pockets on its rear face to reduce weight whilst providing the necessary strength and stiffness. The rear face of the frame is the internal face of fuel tanks 7 and 8 and had the remnants of protective Polymethacrylamide (PMA) foam blocks, adhesive and sealant covering most of it. On the left hand side of the frame one section of the foam cavity protection had been noted on initial inspection as being stained and misshaped Figure 1(a and b). On inspection of the section of frame beneath from where it was removed Figure 1(c) deep pitting corrosion was evident, pitting corrosion was also visible lower down Figure 1(d). Figure 1(e) shows an example of the corrosion. Figure 1(f) shows an area of mechanical damage which was visible on both the LH and RH sides of the frame.

The full teardown inspection of Frame X11185 and Frame X10910 splice revealed numerous findings. The support plates had multiple cracks detected by both visual and NDT inspection. A detailed failure investigation determined these to be caused by fatigue. Corrosion was also widespread with deep pitting corrosion found on the rear of Frame X11185 beneath the PMA foam protection blocks from the internal fuel tanks; this was found to have penetrated to a maximum depth of 2.5mm (27.8%) through the Frame which was measured to be 9mm thick. There were also numerous random areas of light corrosion over the sample areas.

Mechanical damage was widespread over the sample area components and in the case of gouging on the LH rear face of Frame X11185 Figure 11 was found to be quite severe. In this and most cases the damage was found to be due to poor trade practice. Fretting was also quite common, particularly on the interfaces on the forward face of Frame X11185.

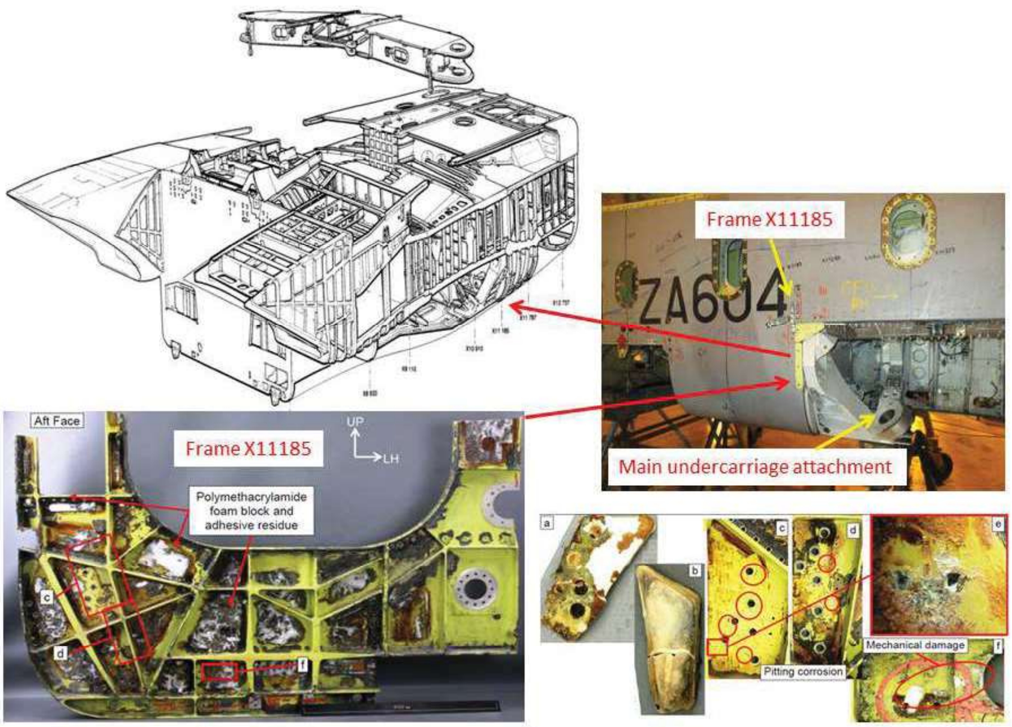

Figure 1: LH Frame X11185 and (a, b) PMA foam block (c - e) corrosion (f) mechanical damage

9 Developments in fatigue, usage and structural health monitoring

9.1 Verification of the RAF C-130J Structural Health Monitoring system through Operational Loads Measurement

S. Dosman and A. Navarrete, Marshall Aerospace and Defence Group, UK

The full paper on this topic can be found in the ICAF 2017 proceedings.

9.1.1 Introduction

Structural Health Monitoring (SHM) systems are often used on missionised aircraft in order to track individual usage against design life, to schedule usage related inspections, and to monitor for changes in usage severity. These systems are generally quite complex and commonly use available parametric data to predict the actual aircraft loading environment before using this data to predict fatigue or damage tolerance related usage. The RAF C-130J aircraft have such an OEM designed SHM system installed, which has been refined several times over its period in service. The latest version upgrade to SHM 7 is now installed on the RAF fleet, and as part of the verification process1 the Operational Loads Monitoring (OLM) systems, which are installed on two of the RAF fleet aircraft, have been used to compare the SHM parametric based results with OLM measured results. The goal of this work is to establish whether further factors on the SHM results are warranted to assure an acceptable level of accuracy in the usage predictions.

9.1.2 Objectives

The objective of the underlying work is the confirmation that SHM is adequately capturing the effect of the loading environment for the full range of RAF flying activities (Operational, ab-initio conversion training, routine flying for currency and training, exercises, etc). The SHM/OLM comparisons cannot provide a full verification, but arguably this is the most important aspect. Given the sensitivity of the data in question the paper will not provide the results of the verification, but it will cover the methodologies used and attempt to gauge their success.

9.1.3 Conclusions

Examples of output can be seen in figures 1 and 2. It can be seen that SHM reported stresses and OLM reported stresses match remarkably well considering the different pedigree of their underlying loads. There are flights where the matches are less close, but on the whole the tie up is extremely good between the two systems.

The first iteration of the work found excessive variability in OLM vs. SHM cross-plot results; however once an improved data set was identified, then much of the variability issues were significantly reduced. This highlights the need for appropriate data for comparisons in these situations.

---

[1] As per RA5720(3), ref [1], which requires that threats to Structural Integrity (SI) are monitored and countered, and RA1220(4), ref [2], which requires that the RAF carry out independent technical evaluation of its safety management systems.

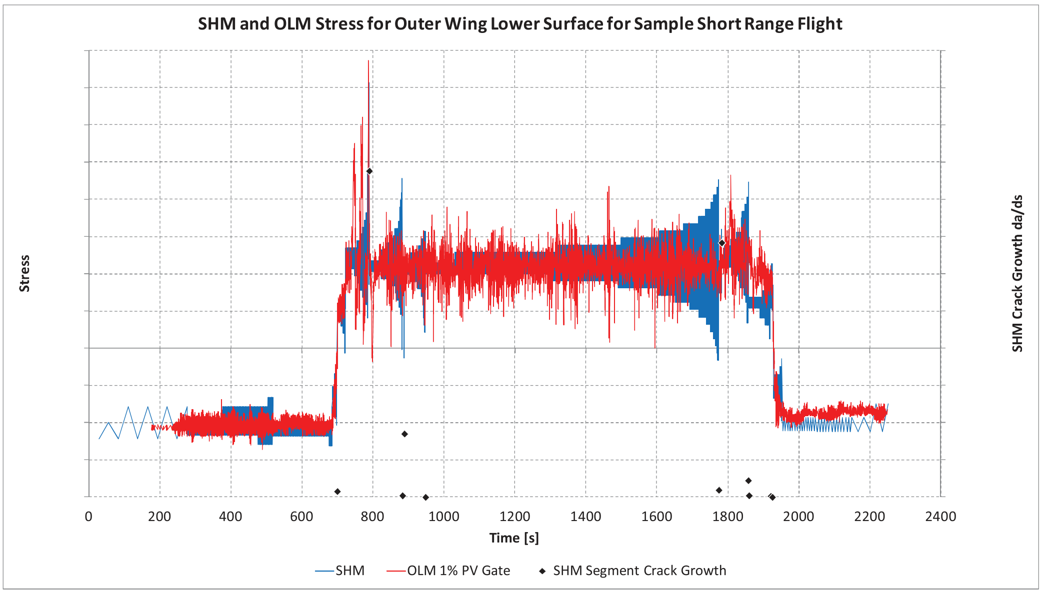

Figure 1 – SHM predicted versus OLM measured results (SHM results reordered within flight segments)

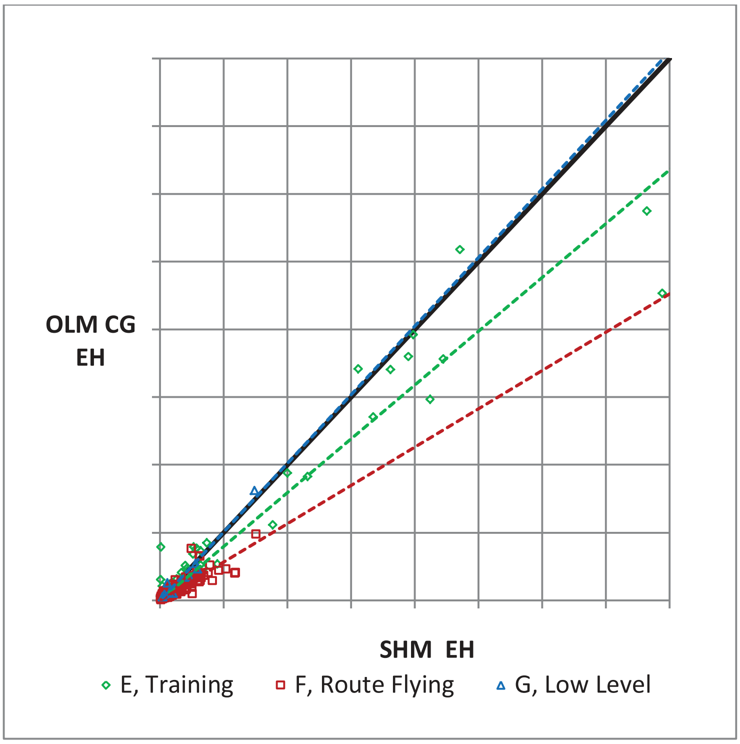

Example Lower Surface Location	E, Training	F, Route Flying	G, Low Level
OLM EH to SHM EH Slope	0.79	0.57	1.01
R^2	0.929	0.768	0.957
95% confidence bound (+-)	0.05	0.03	0.20
(ΣOLM EH) / (ΣSHM EH) Ratio	0.89	0.66	0.97

Figure 2: Cross-plot OLM vs SHM Usage Predictions for Figure 1 location

Adjustments to the SHM reported flight severity are recommended. For the C-130J SHM system it was found that significantly increased accuracy would not be achieved by breaking flight types down into different flying regimes before applying any correction factors; i.e. a single factor per control point is considered adequate.

9.1.4 Innovative Steps

- Use of cross plots to confirm consistency of results before applying corrections (including the use of confidence bounds, and comparisons of cross-plot slope with the simple EH ratio)
- Use of a known loads model to query a loads model with unknown elements and the measures to address these difficulties

9.1.5 Significance

- Demonstrates that SHM assessments can be made even if all the details of the SHM model are unknown (essentially provides what answer would SHM give if it had used the known model)
- Demonstrates consistency of results can be achieved once a sufficient data set is identified
- Demonstrates the relatively accuracy achievable with a parametric based SHM system

[1] RA5720, “Structural Integrity Management”, Military Aviation Authority, Issue 4, 25/08/16.
[2] RA1220, “Project Team Airworthiness and Safety”, Military Aviation Authority, Issue 3, 29/06/15.

9.2 Active training data selection for Gaussian processes designed to predict loads on aircraft landing gear from other in-flight measurements.

G. Holmes[1], A. Thomas[2], W. Capener[2], K. Worden[1], E. Cross[1], [1]The University of Sheffield, United Kingdom [2]Safran Landing Systems UK Ltd, United Kingdom

This is a summary. The full content of this paper can be found in the ICAF2017 proceedings.

The structural health and integrity of aircraft landing gear is a non-negotiable aspect of aircraft design. In the realm of passenger aircraft, zero damage tolerance is enforced, with the result that inefficiencies of over-servicing and reduced lifespan must be built in. An important area of research, therefore, is into technology for monitoring landing gear service conditions. This includes methods to identify load history and unusual loading events. Not everything of interest in this regard can be easily measured, nor would it be desirable to do so from an instrumentation perspective. However, previous research has shown the possibility of accurately predicting unknown loads from other measurements that are already available in the flight data recorder or more easily measured by non-intrusive extra sensors. If such predictions can be made with accuracy and confidence, then it may be possible to reduce inefficiency while still in no way compromising safety.

Gaussian process (GP) regression is a powerful and flexible machine learning tool that has previously been used to make these predictions. It allows the creation of data-driven models to predict unknown quantities from a set of known correlates. A downside of GP regression, like any other data-driven model, however, is that the model can only be as good as the data used to train and condition it. Furthermore, the time required to train a GP model grows cubically with the amount of training data used. For a high dimensional nonlinear problem, a large amount of data is required; the training times can therefore become unfeasibly large.

This paper explores a way of mitigating this problem by ensuring that only the most informative data from all that available is used in the training of the GP models. Using all the available data would mean impossibly long training times even with advanced processing power. A blindly even or random sub-sampling of the data ignores the fact that many data points may have identical information content. Therefore, an active sampling is proposed which combines a principle of maximum separation with additional even sampling. By this combination, information from individual data points is maximised whilst information about the global distribution of the data is also maintained.

The active data selection method is applied to extensive simulated landing datasets, and comparisons are made to alternative data-sampling methods. It is shown that the method allows accurate predictions to be made with less training data and thus within reasonable computational timescales.

9.3 Guidance on integrating matured SHM systems into UK military aircraft

H. Azzam, HAHN Spring Ltd, J. McFeat, BAE SYSTEMS

The UK Military Aviation Authority became aware of the international efforts of the SAE G-11 SHM technical committee. The Committee's first work was a published Aerospace Recommended Practice paper for civil transport aircraft. Whilst the Committee has planned an international military version of the paper, the progress on the paper is anticipated to be slow because the military regulations and standards required for designing and managing aircraft structures can vary between nations and between the military operators of one nation. Therefore, it was suggested that a paper could take benefit from existing work and include contents covering the UK military perspective to provide a good opportunity for peer reviews. This paper provides an overview of the UK perspective and does not promote or endorse a technology or a system; the paper only provides guidance on best practice processes required to integrate a matured SHM technology/system into UK military aircraft. This paper was produced as Military Aircraft Structures Airworthiness Advisory Group (MASAAG) Paper 123 and has been endorsed following peer review and is now published on the UK Government Website (www.uk.gov), under MASAAG Papers.

9.4 Guidance on helicopter operational data recording programmes

S. Reed[1], G. Terry[2] and B. Perrett[3], [1]Dstl, [2]RAE Structures and [3]Helisac Ltd

The experience gained in undertaking helicopter usage validation programmes (see helicopter entries in Section 9) has been included in the development of MASAAG Paper 120 – Guidance on Operational Data Recording Programmes. The latest draft [1] will be circulated to the MASAAG for peer review in May 2017. The aim is have an endorsed paper completed by the end of 2017. This will then by published on the UK Government Website (www.gov.uk), as MASAAG Paper 120.

[1] Reed, S. C., Terry, G. K., and Perrett, B. H. E., Guidance on Operational Data Recording Programmes, Military Aircraft Structural Airworthiness Advisory Group (MASAAG) Paper 120, to be published.

9.5 Rotary-wing aircraft structural usage validation

B. Perrett[1] and S. Reed[2], [1]Helisac, [2]Dstl

The aim of this programme is to describe the usage of helicopters for comparison with Design Usage Spectra (DUS), primarily utilising a Flight Condition Recognition (FCR) approach. The approach is initially to use this method for Statement of Operating Intent and Usage (SOIU) validation and then to extend the approach to cover the vast majority of an Operational Data Recording (ODR) requirement, as detailed in Military Aviation Authority Regulatory Article 5720 – Structural Integrity Management.

The main body of the work has been undertaken by Helisac in a collaborative programme with Leonardo Helicopters (LH) (formerly AgustaWestland) and the Lynx-Wildcat MOD Project Team. Parametric data from the Health and Usage Monitoring System (HUMS)/ Flight Data Recorder (FDR), fitted to the Wildcat Flight Load Survey (FLS) aircraft, have been used to describe the flight conditions flown during the loads survey. Refinement of the Flight Condition Recognition (FCR) algorithms has been undertaken in collaboration with LH, using their definitions of the entry and exit criteria for flight conditions [1]. A programme to use this approach to validate in-service usage of the fleet, by converting the SOI into an SOIU is underway. Over 1600 sorties / 2700 flying hours of in-service data from 59 aircraft in the fleet has been input into the programme and these data will be analysed over the next 6 months.

A similar approach is being run in parallel on the Puma Mk2 fleet, in collaboration with the MOD Project Team and Airbus Helicopters.

In addition, a collaborative programme has been completed by Dstl to validate the SOIU, using FCR, for several of the MOD Special Projects helicopter fleets. Time in flight condition and the event count were identified for the Squirrel (Figure 1) helicopter fleet, using 1767 flying hours / 1239 sorties of data from July 2014 to September 2015. The data were captured from six aircraft instrumented with the Appareo Vision100 data acquisition units. This programme is presented in greater detail in the ICAF2017 proceedings.

Figure 1: MOD Squirrel helicopter

[1] Perrett, B. H., Flight Condition Recognition Software for Operational Data Analysis and Fleet Management, HS-017-A01, March 2017.

9.6 Fixed-wing aircraft structural usage validation

S. Reed, Dstl

Dstl has developed a low-cost structural usage data capture system, based upon commercially-available, Micro Electro Mechanical System (MEMS) technology, for fixed-wing platforms where there is no flight data system fitted. The Modular Signal Recorder (MSR) is a match-box sized self-contained unit that places a very low burden on front-line maintenance crews. In addition, Dstl has developed a universal Aircraft Data Analysis and Monitoring system (ADAM) for analysing flight data from a range of acquisition systems (including the MSR).

The MSR / ADAM approach has been used this year to support data capture and analysis for the following:

- Islander and Defender – 456 flying hours / 295 flights of MSR data from the Islander Mk1 and Defender aircraft (Figure 1) from 2015-2016 were extracted and processed and passed to QinetiQ Farnborough for comparison with previously recorded data [1].

Figure 1: Islander (top) and Defender (bottom) aircraft

- Swordfish – 37 flying hours / 39 sorties of Royal Navy Historic Flight (RNHF) Swordfish (Figure 2) MSR data, representing 100% of flying for the 2016 were analysed and compared with previously recorded data [2]. A total of 167 flying hours of Swordfish data have now been analysed since 2012.

Figure 2: Swordfish aircraft

- Spitfire – 179 flying hours / 208 sorties of Battle of Britain Memorial Flight (BBMF) Spitfire flying from five aircraft over the 2016 season was extracted and processed into flight-by-flight cycle files [3]. These data were passed to Cranfield Aerospace Solutions (CAeS) for use in further fatigue analysis.

- Hurricane – 136 flying hours / 146 sorties of Battle of Britain Memorial Flight (BBMF) Hurricane flying from the two aircraft over the 2016 season was extracted and processed into flight-by-flight cycle files [4]. These data were passed to Cranfield Aerospace Solutions (CAeS) for use in further fatigue analysis. This represented 100% of flying for the 2016 season.

- King Air B200 – MSRs have been fitted to three aircraft in the King Air B200 fleet, under a rolling programme, at RAF Cranwell for approximately a year. In excess of 1000 flying hours of data have been recorded to date. Data capture has now ceased and analysis will be completed by June 2017. During the programme, the MSR data have been used to support investigations into overstress and low-g manoeuvres (e.g. stalls).

The ADAM system has also been developed to capture flight data for structural usage validation (SOIU / OLM) from existing flight data systems for the Sentinel fleet (in collaboration with QinetiQ). A total of 3737 flying hours / 573 sorties of Sentinel data from across the fleet flown between January 2014 and January 2016 were used to validate the vast majority of all of the structural usage design usage assumptions for the Sentinel fleet [5].

[1] Reed, S. C., Islander and Defender Operational Usage Validation Programme – Deliverable 2 – Islander Mk1 and Defender ZH004 MSR Data Analysis, Dstl/708779, 17 March 2017.

[2] Reed, S. C., Fairey Swordfish W5856 – Structural Usage Data Analysis Report 2016, Dstl/707498, 6 February 2017.

[3] Reed, S. C., BBMF Spitfire 2016 Season MSR Data, Dstl/707498 V2, 22 February 2017.

[4] Reed, S. C., BBMF Hurricane 2016 Season MSR Data, Dstl/707498, 22 February 2017.

[5] Reed, S. C., Sentinel RMk1 Operational Loads Measurement Programme Phase 1 Report, DSTL/TR098780 V1, 20 December 2016.

Initial distribution

1.	ICAF2017	
2.	Contributors	
3.	Dstl KIS	Athena

Report documentation page **v3.0**

1a.	**Report number:** DSTL/TR102138		1b.	**Version number:** Ver 2	
2.	**Date of publication:** 27/04/2017		3.	**Number of pages:** iiii + 58	
4a.	**Report UK protective marking:** OFFICIAL				
4b.	**Report national caveats:**				
4c.	**Report descriptor:**				
5a.	**Title:** Review of aeronautical fatigue and structural integrity investigations in the UK during the period April 2015 - April 2017				
5b.	**Title UK protective marking:** UNLIMITED				
5c.	**Title national caveats:**				
5d.	**Title descriptor:**				
6a.	**Alternate title:**				
6b.	**Alternate title UK protective marking:**				
6c.	**Alternate title national caveats:**				
6d.	**Alternate title descriptor:**				
7.	**Authors:** Reed, S.C. and Hallam, D.				
8.	**Name and address of publisher:** Dstl Platform Systems Division Porton Down Salisbury Wilts SP4 0JQ		9.	**Name and address of sponsor:** - -	
10.	**Sponsor contract:** -				
11.	**Dstl project number:** -				
12.	**Work package number:**				
13.	**Other report numbers:**				
14a.	**Contract start date:**		14b.	**Contract end date:**	
15a.	**IPR:**				
15b.	**Patents:** NO				
15c.	**Application number:**				

16a.	**Abstract:**			
	This report provides a review of the aeronautical fatigue and structural integrity investigations carried out in the UK during the period April 2015 to April 2017.			
16b.	**Abstract UK protective marking:**		UNLIMITED	
16c.	**Abstract national caveats:**			
16d.	**Abstract descriptor:**			
17.	**Keywords:**			
	Aeronautical fatigue, structural integrity, ICAF			
18.	**Report announcement and availability**			
	Announce to	Available to		
18a.	☒	☒	UK MOD has unlimited distribution rights	
18b.	☒	☒	UK MOD has no rights of distribution	
18c.	☒	☒	Can be distributed to UK MOD and its agencies	
18d.	☒	☒	Can be distributed to all UK government departments	
18e.	☒	☒	Can be distributed to all UK defence contractors	
18f.	☒	☒	Can be distributed to all foreign government departments	
18g.	**Additional announcement:**			
18h.	**Additional availability:**		International Committee on Aeronautical Fatigue and Structural Integrity - 2017	
18i.	**Release authority role:**			

THIS PAGE INTENTIONALLY LEFT BLANK